



UPPSALA  
UNIVERSITET

*Digital Comprehensive Summaries of Uppsala Dissertations  
from the Faculty of Science and Technology 1001*

# Characterization of Reaction Products in the Li-O<sub>2</sub> Battery Using Photoelectron Spectroscopy

REZA YOUNESI



ACTA  
UNIVERSITATIS  
UPSALIENSIS  
UPPSALA  
2012

ISSN 1651-6214  
ISBN 978-91-554-8544-3  
urn:nbn:se:uu:diva-183887

Dissertation presented at Uppsala University to be publicly examined in Polhemsalen, Ångström Laboratory, Lägerhyddsvägen 1, Uppsala, Wednesday, December 19, 2012 at 10:15 for the degree of Doctor of Philosophy. The examination will be conducted in English.

#### **Abstract**

Younesi, R. 2012. Characterization of Reaction Products in the Li-O<sub>2</sub> Battery Using Photoelectron Spectroscopy. Acta Universitatis Upsaliensis. *Digital Comprehensive Summaries of Uppsala Dissertations from the Faculty of Science and Technology* 1001. 65 pp. Uppsala. ISBN 978-91-554-8544-3.

The rechargeable Li-O<sub>2</sub> battery has attracted interest due to its high theoretical energy density (about 10 times better than today's Li-ion batteries). In this PhD thesis the cycling instability of the Li-O<sub>2</sub> battery has been studied. Degradation of the battery has been followed by studying the interface between the electrodes and electrolyte and determining the chemical composition and quantity of degradation products formed after varied cycling conditions. For this in-house and synchrotron based Photoelectron Spectroscopy (PES) were used as a powerful surface sensitive technique. Using these methods quantitative and qualitative information was obtained of both amorphous and crystalline compounds. To make the most realistic studies the carbon cathode pore structure was optimised by varying the binder to carbon ratio. This was shown to have an effect on improving the discharge capacity. For Li-O<sub>2</sub> batteries electrolyte decomposition is a major challenge. The stability of different electrolyte solvents and salts were investigated. Aprotic carbonate and ether based solvents such as PC, EC/DEC, TEGDME, and PEGDME were found to decompose during electrochemical cycling of the cells. The carbonate based electrolytes decompose to form a 5-10 nm thick surface layer on the carbon cathode during discharge which was then removed during battery charging. The degradation products of the ether based electrolytes consisted mainly of ether and carbonate based surface species. It is also shown that Li<sub>2</sub>O<sub>2</sub> as the final discharge product of the cell is chemically reactive and decomposes carbonate and ether based solvents. The stability of lithium electrolyte salts (such as LiPF<sub>6</sub>, LiBF<sub>4</sub>, LiB(CN)<sub>4</sub>, LiBOB, and LiClO<sub>4</sub>) was also studied. The PES results revealed that all salts are unstable during the cell cycling and in contact with Li<sub>2</sub>O<sub>2</sub>. Decomposition layers thinner than 5 nm were observed on Li<sub>2</sub>O<sub>2</sub>. Furthermore, it is shown that the stability of the interface on the lithium anode is a chief issue. When compared to Li batteries (where oxygen levels are below 10 ppm) working in the presence of excess oxygen leads to the decomposition of carbonate based electrolytes to a larger degree.

*Keywords:* Li-O<sub>2</sub> Battery, Surface Characterization, Lithium-Air Battery, Photoelectron Spectroscopy, XPS

*Reza Younesi, Uppsala University, Department of Chemistry - Ångström, Box 523, SE-751 20 Uppsala, Sweden.*

© Reza Younesi 2012

ISSN 1651-6214

ISBN 978-91-554-8544-3

urn:nbn:se:uu:diva-183887 (<http://urn.kb.se/resolve?urn=urn:nbn:se:uu:diva-183887>)

*To those people who try to make a  
better world.*

*To those people who work for the  
freedom of everyone.*





# List of Papers

This thesis is based on the following papers, which are referred to in the text by their Roman numerals.

- I **Younesi, S. R.**, Urbonaite, S., Björefors, F., Edström, K., (2011) Influence of the cathode porosity on the discharge performance of the lithium–oxygen battery. *Journal of Power Sources*, 196, 9835–9838.
- II **Younesi, R.**, Hahlin, M., Treskow, M., Scheers, J., Johansson, P., Edström, K., (2012) Ether Based Electrolyte, LiB(CN)<sub>4</sub> Salt and Binder Degradation in the Li–O<sub>2</sub> Battery Studied by Hard X-ray Photoelectron Spectroscopy (HAXPES). *The Journal of Physical Chemistry C*, 116, 18597–18604.
- III **Younesi, R.**, Hahlin, M., Björefors, F., Johansson, P., Edström, K., Li-O<sub>2</sub> Battery Degradation by Lithium Peroxide (Li<sub>2</sub>O<sub>2</sub>): a model study. *Submitted*.
- IV **Younesi, R.**, Urbonaite, S., Edström, K., Hahlin, M., (2012) The Cathode Surface Composition of a Cycled Li-O<sub>2</sub> Battery: a Photoelectron Spectroscopy Study. *The Journal of Physical Chemistry C*, 116, 20673–20680.
- V **Younesi, R.**, Hahlin, M., Edström, K., Surface Characterization of the Carbon Cathode and Lithium Anode of Li-O<sub>2</sub> Batteries using LiClO<sub>4</sub> or LiBOB salts. *Submitted*.
- VI **Younesi, R.**, Hahlin, M., Roberts, M., Edström, K., (2013) The SEI Layer Formed on Lithium Metal in the Presence of Oxygen: A Seldom Considered Component in the Development of the Li-O<sub>2</sub> battery. *Journal of Power Sources*, 225, 40-45.

Reprints were made with permission from the respective publishers.

Additional papers not included in this thesis:

1. **Younesi, R.**, Roberts, M., Edström, K., The Instability of Ether Based Electrolytes in the Li-O<sub>2</sub> Battery. *Nature Chemistry*, submitted on 7<sup>th</sup> of Sep., 2012.
2. **Younesi, R.**, Singh, N., Urbonaite, S., Edström, K., (2010) The Effect of Pore Size on the Performance of the Li-O<sub>2</sub> battery. *ECS Transactions*, 25, 121–127.
3. Asfaw, H., Roberts, M., **Younesi, R.**, Edström, K., Advanced 3D Structured Batteries Fabricated Using Emulsion Templated High Surface Area Carbon Foams. *Submitted*.

Comments on my contribution to the appended papers in this thesis:

**I** Major part of the experimental work. Part of the writing.

**II** Major part of the experimental work and analysis of results. Main author of the paper.

**III** Planning most of the work. Major part of the experimental work and analysis of results. Main author of the paper.

**IV** Planning some part of the study. Major part of the experimental work. Part of the writing.

**V** Planning most of the work. Major part of the experimental work and analysis of results. Main author of the paper.

**VI** Planning most of the work. Major part of the experimental work and analysis of results. Main author of the paper.

# Contents

1. Introduction.....	11
1.1. Renewable Energies .....	11
1.2. Lithium Batteries .....	12
1.3. The Scope of this Thesis .....	13
Historical Background of this Thesis.....	13
Methodology.....	14
2. The Li-O <sub>2</sub> Battery .....	15
The Discharge Capacity.....	15
The ORR and OER Reactions .....	16
The Cathode.....	17
The Electrolyte .....	18
The Anode .....	19
The State of the Art.....	19
3. Experimental.....	21
3.1. The Cell Setup.....	21
3.2. Characterization of the Electrodes .....	22
Photoelectron Spectroscopy.....	22
4. Summary of Results and Discussion.....	26
4.1. Cathode.....	26
The Effects of Cathode Porosity.....	26
Binder Decomposition.....	29
Chemical Stability of Cathode Components.....	30
Summary of Studies on Cathode .....	32
4.2. Electrolyte Solvent.....	33
The Cycling Performance of Carbonate Electrolytes .....	33
Chemical Decomposition of Carbonate Solvents by Li <sub>2</sub> O <sub>2</sub> .....	37
The Cycling Performance of Ether Electrolytes .....	39
Chemical Decomposition of Ether Solvents by Li <sub>2</sub> O <sub>2</sub> .....	41
Summary of Studies on Electrolyte Solvents .....	42

4.3. Electrolyte salt.....	43
4.3.1. Stability of Li Salts during Cell Cycling .....	43
4.3.2. Stability of Li Salts in Contact with $\text{Li}_2\text{O}_2$ .....	46
Summary of Studies on Li Salts .....	48
4.4. Anode .....	49
5. Concluding Remarks and Future Outlook .....	53
Sammanfattning på Svenska .....	56
Acknowledgements.....	60
References.....	62

# Abbreviations

EC/DEC	Ethylene carbonate/diethyl carbonate
CV	Cyclic Voltammetry
DME	Dimethoxyethane
HAXPES	Hard X-ray Photoelectron Spectroscopy
ORR	Oxygen reduction reaction
OER	Oxygen evolution reaction
PC	Propylene carbonate
PEGDME	Polyethylene glycol dimethyl ether
PES	Photoelectron Spectroscopy
PSD	Pore Size Distribution
SEI	Solid Electrolyte Interphase
SEM	Scanning Electron Microscopy
TEGDME/Tetraglyme	Tetraethylene glycol dimethyl ether
XPS	X-ray Photoelectron Spectroscopy



# 1. Introduction

## 1.1. Renewable Energies

The demand to develop renewable energies to reduce fossil fuel consumption has been increasing in recent years. Global warming as a result of greenhouse gas emissions is one of the chief concerns motivating investment in renewable energies to replace fossil fuels. In the year 2000 the annual CO<sub>2</sub> emission from the combustion of fossil fuels surpassed 6.7 Gt C (gigatonne of carbon)<sup>1</sup>, and thus, to protect the earth's atmosphere and minimize global warming many countries have presented plans to reduce greenhouse gas emissions (*e.g.* the EU has planned for an 80% reduction in its 1990 greenhouse gas emissions by the year 2050).<sup>2</sup> In these plans, a primary goal is the development of renewable energies for transport. According to the energy policy in Sweden, 10% of the energy required in the transport sector shall be provided by renewable energies by the year 2020.<sup>3</sup> Similarly, the EU has recently proposed a plan to reduce transport emissions to 60% of their current value by the year 2050. To achieve this goal, several targets have been defined such as:

*“No more conventionally-fuelled cars in cities”*.<sup>2</sup>

Another major factor in the drive for renewable energy is the instability of oil prices and sources in the future. The dependency of many countries on oil (which is located in only a few areas) is a threat to the world economy as well as to world peace.<sup>4</sup> In addition, the abuse of power resulting from economies driven by oil import and export has affected the lives of many people in many countries across the world.

Therefore, considering the troubles originating from this huge consumption of fossil fuels, further developments are required to lead societies to a future powered by renewable energies. In such a development, advanced energy storage technologies such as batteries play a key role, especially as they can be combined with sustainable energy systems such as wind, solar and hydro power. Key to the realisation of this future is efficient energy storage and the most realistic solution is the battery.

A battery or an electrochemical cell is made of electrodes and electrolyte, which converts chemical energy into electrical energy. Already in ~200 BC in the Parthian era a battery called the “Baghdad Battery” produced of a copper cylinder and iron rod was used, although it is not clear in what appli-

cation this battery was used.<sup>5,6</sup> However, the real birth of battery technology is attributed to the development in 1800 by Alessandro Volta of the voltaic pile.<sup>6</sup> Since then, hundreds of different chemical reactions have been utilized to create battery systems including the development of lithium batteries in 1990.<sup>7</sup>

## 1.2. Lithium Batteries

The modern lithium battery which is well adapted nowadays in all portable electronic devices is the result of years of effort by the scientific community. These so called “Li-ion batteries” operate via the use of insertion or intercalation electrodes which can host  $\text{Li}^+$  ions in their structure.<sup>8</sup> Many different electrode materials have been investigated for both the anode and cathode of Li-ion batteries. However, the most commercially available Li-ion batteries are assembled using a graphite based anode and a metal oxide based cathode. Figure 1 shows a schematic illustration of a Li-ion battery during the discharge of the cell when Li ions deintercalate from the negative electrode and intercalate into the positive electrode simultaneously. This is the discharge of the cell. During the charge, the reverse reactions occur on the electrodes.

Further development of Li-ion batteries focusses on increasing the specific energy (gravimetric energy density) and the energy density (volumetric energy density) to fulfill the increased consumer demands especially for electric vehicles.

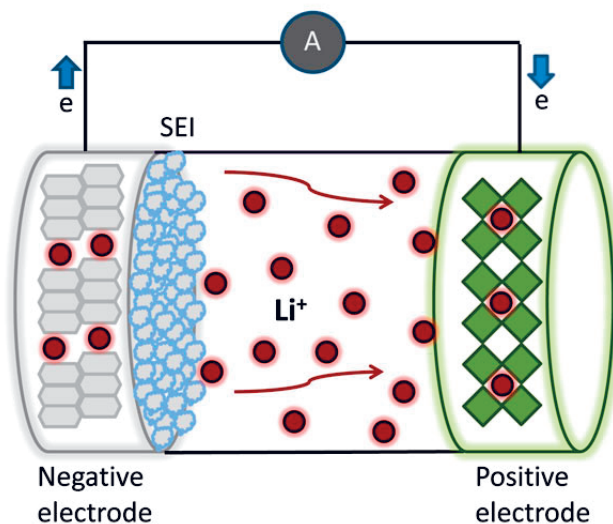


Figure 1. A schematic drawing of a Li-ion battery with two insertion electrodes.



In this respect, the Li-O<sub>2</sub> battery has attracted attention in recent years due to its high specific energy.<sup>9</sup>

This type of battery possesses a theoretical specific capacity almost 10 times higher than that of Li-ion batteries. However, it is predicated a practical Li-O<sub>2</sub> cell will provide a specific capacity 2-3 times higher compared to that of commercially available Li-ion batteries (Figure 2).<sup>9,10</sup> The Li-O<sub>2</sub> battery is comprised of a metallic lithium anode (or possibly lithium alloy) and a porous cathode, where the oxygen fuel is consumed.

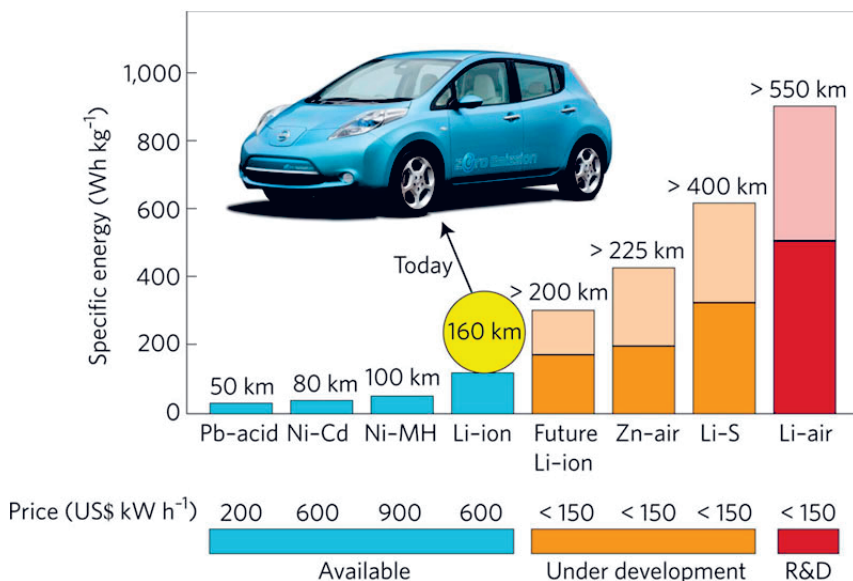


Figure 2. Estimated practical specific energies for some rechargeable batteries with estimated driving distances and pack prices. Reprinted with permission from ref<sup>9</sup>.

### 1.3. The Scope of this Thesis

#### Historical Background of this Thesis

This PhD study started in 2008 with the goal to study the rechargeability of the Li-O<sub>2</sub> battery. At that time no work was published regarding the decomposition of electrolytes. Hence, one of the main steps in this research was to evaluate the formation of the proposed discharge products, Li<sub>2</sub>O<sub>2</sub> and/or Li<sub>2</sub>O, and to check the stability of the electrolyte. Initially carbonate based electrolytes such as propylene carbonate (PC) and ethylene carbonate/diethyl carbonate (EC/DEC) were used because they were the most common ones. In 2009-2010 studies showed that these types of electrolytes were unstable at the air cathode during cycling of the battery, and consequently ether based electrolytes were proposed. Thus, the performance of a battery cycled with a

tetraethylene glycol dimethyl ether (TEGDME) based electrolyte was studied in this thesis. In addition, the stability of a polyethylene glycol dimethyl ether (PEGDME) based electrolyte was studied for the first time for the Li-O<sub>2</sub> battery. Furthermore, the stability of common lithium salts was investigated, which was an untouched aspect of research when the study started.

Since the improvement of Li-O<sub>2</sub> batteries has been hampered due to the instability of electrolytes, the main goal of this study was to elucidate the processes taking place during the discharge and charge both the intended oxygen reduction and oxygen evolution reactions (ORR and OER) and the parallel parasitic electrochemical and chemical reactions.

Despite that today it is well known that the stability of electrolytes in contact with the intermediate and final discharge reaction products of the Li-O<sub>2</sub> battery is a chief issue, the stability of the electrolyte in contact with the Li anode in the presence of oxygen has up until now been neglected. As a part of this thesis, this issue was also studied.

## Methodology

In this thesis, the Li-O<sub>2</sub> battery was studied to elucidate the complicated parameters influencing the system. The thesis includes results of studies of the three main cell components *i.e.* cathode, anode and electrolyte. In a wider sense understanding the reactions and determining the reaction products in this novel battery system have been the scope of this thesis.

Several characterization techniques including scanning electron microscopy (SEM), X-ray diffraction (XRD), and Gas Adsorption have been used to analyze the cell electrodes along with electrochemical measurement of the Li-O<sub>2</sub> cells. However, in-house and synchrotron-based photoelectron spectroscopy (PES) was used as the main characterization tool to study the surfaces of cathode and anode of the cells.

The PES measurements were performed at two different large scale synchrotron facilities using different photon energies. The results obtained in synchrotron facilities were also used as a depth profiling technique.

## 2. The Li-O<sub>2</sub> Battery

The Li-O<sub>2</sub> battery has often been called Li-air (or lithium-air) battery assuming that the battery consumes oxygen from the ambient atmosphere. However, due to the difficulties to exclude incoming moisture and nitrogen from the atmosphere to the battery, production of a rechargeable lithium-air battery is impossible with today's knowledge.

Therefore, the rechargeability of the Li-O<sub>2</sub> system has so far been investigated using only a pure oxygen atmosphere. Below some important aspects of the Li-O<sub>2</sub> battery are presented.

### The Discharge Capacity

The Li-O<sub>2</sub> battery possesses a very high specific energy (gravimetric energy density) originating from the use of lithium metal as the negative electrode and the consumption of gaseous oxygen from the atmosphere at the positive electrode (Figure 3).

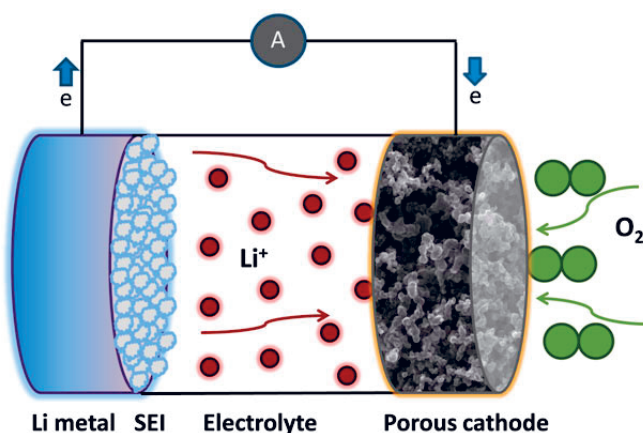


Figure 3. A schematic picture of the Li-O<sub>2</sub> battery.

Lithium is the lightest metal providing a specific capacity of 3861 mAh/g which is much greater than that of graphite or other commercially available anodes.<sup>10</sup> In the Li-O<sub>2</sub> battery with a nonaqueous electrolyte, reactions between reduced oxygen and lithium ions results in the formation of lithium peroxide (Li<sub>2</sub>O<sub>2</sub>) (or possibly lithium oxide (Li<sub>2</sub>O)) as the final discharge

reaction product in the cathode pores. The total amount of Li that can be stored in  $\text{Li}_2\text{O}_2$  or  $\text{Li}_2\text{O}$  in the porous cathode is much greater than that in intercalation cathodes like  $\text{LiCoO}_2$  (the theoretical specific energy of today's Li-ion batteries and a nonaqueous Li- $\text{O}_2$  battery are 387 and 3582 Wh  $\text{kg}^{-1}$ ).<sup>9</sup>

## The ORR and OER Reactions

Acquiring a truly reversible oxygen reduction and oxygen evolution reactions (ORR and OER) resulting in the formation and oxidation of  $\text{Li}_2\text{O}_2$ , respectively, is the key point in the Li- $\text{O}_2$  battery. The rechargeability of the Li- $\text{O}_2$  battery using nonaqueous electrolytes was first proposed by Abraham and Jiang in 1996.<sup>11</sup> Later from 2006 to 2008, Bruce et al. reported promising results claiming 50 cycles for Li- $\text{O}_2$  cells.<sup>12-14</sup> Since then, there have been vast efforts to improve the performance of the Li- $\text{O}_2$  battery to retain the cell capacity after repeated cycles. However, a cell with a couple of hundred rechargeable cycles has not been achieved yet.

Three possible reactions between  $\text{Li}^+$  and reduced oxygen have been considered:<sup>11,12,15,16</sup>



However, it has been suggested that gaseous oxygen dissolved in the electrolyte first via a one electron transfer process reduces at the surface of a porous cathode to a super oxide ion ( $\text{O}_2^-$ ). This reduced oxygen ion reacts with  $\text{Li}^+$  ions dissolved in the electrolyte to form lithium superoxide ( $\text{LiO}_2$ ) as the intermediate reaction product.  $\text{LiO}_2$  can further chemically or electrochemically be converted to lithium peroxide ( $\text{Li}_2\text{O}_2$ ) as the final discharge reaction product:<sup>15</sup>



It has been suggested that during the reverse process (cell charging),  $\text{Li}_2\text{O}_2$  oxidizes as:<sup>15</sup>



It is expected to observe a higher voltage in the OER than in the ORR. Results published in the literature have often shown that the charge plateaus in Li- $\text{O}_2$  cells are usually  $\sim 0.5$ - $1.5$  V higher than the discharge plateaus. This

has been considered as a major drawback for any practical cell. There have been several studies aiming at using catalysts to decrease this hysteresis.<sup>17-20</sup>

## The Cathode

The cathode of the Li-O<sub>2</sub> battery is a porous electrode which can store discharge reaction products. Given that the oxygen solubility and the diffusion coefficient in nonaqueous electrolytes are relatively small and as a consequence so are the kinetics of the discharge reaction, therefore, at a slow discharge rate, the amount of formed Li<sub>2</sub>O<sub>2</sub> and thus the discharge capacity of the cell is mainly limited by the porosity properties of the cathode such as surface area, pore volume, pore size distribution, etc.

So far most of the cathodes used for Li-O<sub>2</sub> cells are made of carbon, binder, and possibly catalyst. Considering the practical ways to produce a cathode, the most common technique is mixing active materials with binder using a solvent to make a slurry, which is then cast onto a mesh or foam as the substrate.<sup>12-14</sup> However, other designs like a binder-free cathode<sup>21,22</sup> and hot-rolled cathode (solvent-free)<sup>23</sup> have also been used.

To increase the discharge capacity of the Li-O<sub>2</sub> battery, several studies have been performed to optimize the porosity properties of the carbon cathode.<sup>24-30</sup> These studies were aiming at improving the formulation of the cathode to provide more space to store higher amounts of Li<sub>2</sub>O<sub>2</sub>. In addition, it has been desired that the increase in the surface area of the cathode will improve the triple boundary between the interface of gaseous O<sub>2</sub>, electrolyte and the cathode. This would accelerate the kinetics of the oxygen reduction and consequently the kinetics of the reaction between reduced oxygen ions and Li<sup>+</sup>. However, the surface area is not the only parameter affecting the cell performance. The studies concluded that other parameters such as pore size distribution (PSD) and pore volume of the cathode, porosity and chemistry of the carbon itself, the electrode thickness, the carbon loading, cathode formulation, etc. influence the discharge capacity and performance of the Li-O<sub>2</sub> battery.<sup>24-30</sup>

Catalysts often have been used as a component of the porous cathode since it is believed that catalysts can improve the kinetics of ORR and OER reactions. They have also been utilized in order to lower the charge overpotential in the cell. The effect of different catalysts including metal oxides (e.g., MnO<sub>2</sub>, Co<sub>3</sub>O<sub>4</sub>), precious metals (e.g., Au and Pt), and nonprecious alloys (e.g., CuFe) on the performance of Li-O<sub>2</sub> cells have been studied.<sup>17-19</sup>

Further works to improve the structure of the cathode in order to increase the discharge capacity and kinetics of the reactions and to synthesize efficient catalysts are somewhat hampered due to the weakness of the available electrolytes for the Li-O<sub>2</sub> battery. Thus, establishing reversible formation and oxidation of Li<sub>2</sub>O<sub>2</sub> is a difficult prerequisite to study and improve the struc-

ture of the cathode properly. The discovery of a stable electrolyte will in the future lead to acceleration in the research on the architecture of the cathode.

## The Electrolyte

$\text{LiO}_2$  and  $\text{Li}_2\text{O}_2$ , as the intermediate and final discharge reaction products of the Li- $\text{O}_2$  battery are chemically very reactive. As a consequence of this fact, most of the known electrolytes are unstable in the Li- $\text{O}_2$  battery.

In the preliminary work (2006-2008) on the development of the Li- $\text{O}_2$  battery, carbonate based electrolytes particularly  $\text{LiPF}_6$  in PC were mainly used.<sup>12-14</sup> However, later works indicated that these types of electrolytes decompose during the cell cycling.<sup>31-33</sup> Several different mechanisms have been proposed for the decomposition of carbonate based electrolytes such as PC. It has been suggested that super oxide radical ( $\text{O}_2^{\bullet-}$ ) reacts via nucleophilic substitution with the C of the carbonyl group in PC.<sup>34,35</sup> It has also been suggested that the super oxide radical attacks the ethereal carbon of PC.<sup>31,36</sup> and that  $\text{Li}_2\text{O}_2$ , which is a strong oxidizing agent, can decompose PC.<sup>37,38</sup> However, all the proposed mechanisms agree that  $\text{O}_2^{\bullet-}$  and/or  $\text{Li}_2\text{O}_2$  via nucleophilic attack, proton/hydrogen abstraction, or electron transfer decompose PC and probably all the other carbonate based solvents.<sup>34-37,39,40</sup> In the lithium salt containing electrolytes, the decomposition of PC results in ring opening of the PC molecule and formation of carbonate based species such as lithium alkyl carbonates and lithium carbonates.<sup>31</sup>

The decomposition of carbonate based electrolytes led to the suggestion to instead use ether based electrolytes.<sup>41,42</sup> Several studies have recently proved that  $\text{Li}_2\text{O}_2$  forms as a discharge product when using ether based electrolytes.<sup>22,41-45</sup> This has raised the hope that the electrolyte instability challenge had been overcome. However, further studies revealed that also ether based electrolytes degrade during the cell cycling.<sup>46-48</sup>

Beside the instability of electrolyte solvents, degradation of lithium salts is also a main issue.<sup>48-50</sup> Several lithium salts including  $\text{LiPF}_6$ ,  $\text{LiB}(\text{CN})_4$ ,  $\text{LiBOB}$ ,  $\text{LiTfSI}$ ,  $\text{LiBF}_4$ ,  $\text{LiClO}_4$ , and  $\text{LiCF}_3\text{SO}_3$  have been investigated for the Li- $\text{O}_2$  battery. Nevertheless, most of these salts decompose during the cell cycling due to the reaction with intermediate products or due to reaction with  $\text{Li}_2\text{O}_2$ .<sup>38,51-53</sup>

Overall, the degradation of the electrolyte solvents and salts in the Li- $\text{O}_2$  battery is still one major challenge, although already many different types of electrolytes including aprotic organic electrolytes, polymer electrolytes, ionic liquids, etc. have been investigated.

## The Anode

The presence of lithium metal as the anode of the Li-O<sub>2</sub> battery implies an extra dilemma in the battery system. The formation and growth of dendrites on lithium metal has been the most common issue when using lithium metal in Li-ion batteries rendering the replacement of lithium by a graphite anode. In addition, lithium is one of the strongest reducing agent with a very negative electrode potential. This means that the contact between lithium and any of the aprotic electrolytes results in partial decomposition of the electrolyte on the lithium and formation of a surface layer so called the solid electrolyte interphase (SEI).<sup>54</sup> The SEI protects the electrolyte from further decomposition by the negative electrode. There have been attempts to suppress dendrite formation and electrolyte decomposition by using additives and solid electrolytes.<sup>55-57</sup> Nevertheless, employment of lithium metal as an anode requires extra care. This is more problematic in the Li-O<sub>2</sub> battery since O<sub>2</sub> and O<sub>2</sub><sup>-</sup> ions are present in the electrolyte solution. It has been suggested that to protect the lithium anode by using a solid state membrane.<sup>58-60</sup> It is also possible to replace lithium anode by silicon or graphite electrodes or even by high voltage electrodes such as LiFePO<sub>4</sub> (not for practical application) to avoid the severe contact between lithium anode, oxygen species and electrolyte.<sup>61,62</sup>

Nevertheless, the chemistry of the SEI on lithium anodes and its functioning during the Li-O<sub>2</sub> cell cycling is seldom considered and is still unidentified in different electrolytes.<sup>63</sup>

## The State of the Art

Overall, the works performed in recent years have shown that the main three cell components, *i.e.* anode, cathode, and electrolyte, suffer from several obstacles including the instability of the electrolyte solvents and salts, synthesis of an efficient catalyst, stability of lithium anode, improving cathode formulation, etc.<sup>17,42,64-68</sup>

In addition to the challenges for each component of the Li-O<sub>2</sub> battery, cross-talk between cell components is a major issue. For example, acetonitrile and DMSO solvents have recently been shown to be relatively stable during the ORR and OER.<sup>69,70</sup> However, the lithium anode is not stable in contact with these two solvents making them inapplicable for the Li-O<sub>2</sub> battery. Another example is that ether solvents such TEGDME or dimethoxyethane (DME) in contact with Li<sub>2</sub>O<sub>2</sub> decompose and in turn the decomposition products degrade Kynar binder of the cathode.

Therefore, all these challenges have resulted in making the Li-O<sub>2</sub> battery a very difficult system to study. Only when truly reversible reactions are achieved without any side reaction will clear fundamental studies and optimization of the cell be possible.

Regarding the surface analysis, it is worth mentioning that to improve the understanding of reactions in batteries, the ambient pressure X-ray photoelectron spectroscopy (APXPS) can be used. This is a relatively newly developed technique which can be used as an in-situ tool to investigate surfaces formed during the cell discharge and charge.<sup>71,72</sup>



### 3. Experimental

In this thesis, different materials to assemble the cell and different analytical techniques to characterize the cell electrodes were used. The details of each work within this thesis are explained in the appended papers (**paper I to VI**). Here overviews of the cells setup and of characterization techniques are briefly described.

#### 3.1. The Cell Setup

Li-O<sub>2</sub> cells were assembled using a modified Swagelok™ cell design with an opening allowing oxygen access to the cathode (Figure 4). In this design, a stainless steel rod and an aluminum hollow rod were used as the current collectors of the negative and positive electrodes, respectively. The cells were assembled in an Argon-filled glove box (O<sub>2</sub>, H<sub>2</sub>O <2 ppm) using lithium foil as the negative electrode, Solupor or glass fibers sheets as separator, and a porous cathode as the positive electrode.

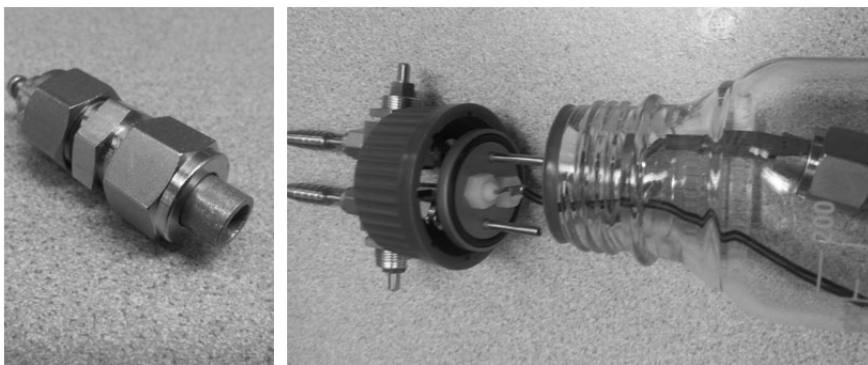


*Figure 4.* Photograph of Swagelok™ cell and a specially designed air-tight container with inlet and outlet valves for oxygen gas purging.

The porous cathodes used had different formulation depending to the aim of the study. The details of the cathode preparations are presented in the appended papers. Generally, the cathodes were made of carbon Super P (Lithium battery grade, Erachem Comilog), Kynar 2801 (Arkema) as binder, with/without  $\alpha$ -MnO<sub>2</sub> as a catalyst. Prior to use, the cathodes were dried at 120°C in a vacuum furnace contained within a glove box.

Several lithium salts such as  $\text{LiPF}_6$ ,  $\text{LiClO}_4$ ,  $\text{LiB}(\text{CN})_4$ ,  $\text{LiBOB}$ , and  $\text{LiBF}_4$  dissolved in different carbonate and ether based solvents including PC, EC/DEC, TEGDME, PEGDME, and DME were used as the electrolyte. The water contents of the electrolytes were measured using Karl Fisher titration.

The cells were kept in specially designed air-tight containers with inlet and outlet valves for oxygen gas purging (Figure 4). The details of the applied current and voltage, which were different for different studies, are mentioned in the appended papers. The applied current and the capacities of the cells were calculated based on the amount of carbon in the cathodes. In most cases the cells were discharged and charged galvanostatically using Digatron BTS-600 applying a current density of 70 mAh/g. However, lower and higher current densities were also tested.

## 3.2. Characterization of the Electrodes

To characterize cathodes or anode materials different techniques including SEM (LEO 1550), XRD (SIEMENS D5000), and nitrogen gas adsorption (Micromeritics ASAP 2020) were used. Along with these techniques, in-house and synchrotron-based PES have been mainly used in this work to characterize the surface of a carbon cathode and also of the lithium anodes from cells.

### Photoelectron Spectroscopy

PES, also known as XPS (X-ray photoelectron spectroscopy) and ESCA (electron spectroscopy for chemical analysis), is a powerful technique to analyze surfaces due to its high surface sensitivity. The strengths of PES also arise from its ability to i) identify and quantify the elemental composition of solid surfaces made of any element from lithium to uranium, and ii) give information about the chemical environment of the elements. These abilities make PES a technique that can provide qualitative and quantitative information about both amorphous and crystalline chemical compounds.

The PES technique is based on the photoelectric effect, this works by electrons (photoelectrons) being emitted from a solid surface if it is irradiated with electromagnetic radiation (photons) above a certain threshold energy. Figure 5 shows a schematic drawing of PES, where an atom is irradiated with a photon resulting in the emission of an electron with a specific kinetic energy. Thus, by measuring the kinetic energy of the photoelectron ( $E_K$ ) and by knowing the photon energy ( $h\nu$ ), the law of conservation of energy tells that the binding energy of photoelectrons can be calculated as following:<sup>73</sup>

$$E_B = h\nu - E_K - \phi \quad (7)$$

where  $E_B$  is the binding energy of electrons of the target atom from which electron originate,  $h\nu$  is the photon energy,  $E_K$  is the kinetic of the emitted electron, and  $\phi$  is the work function.

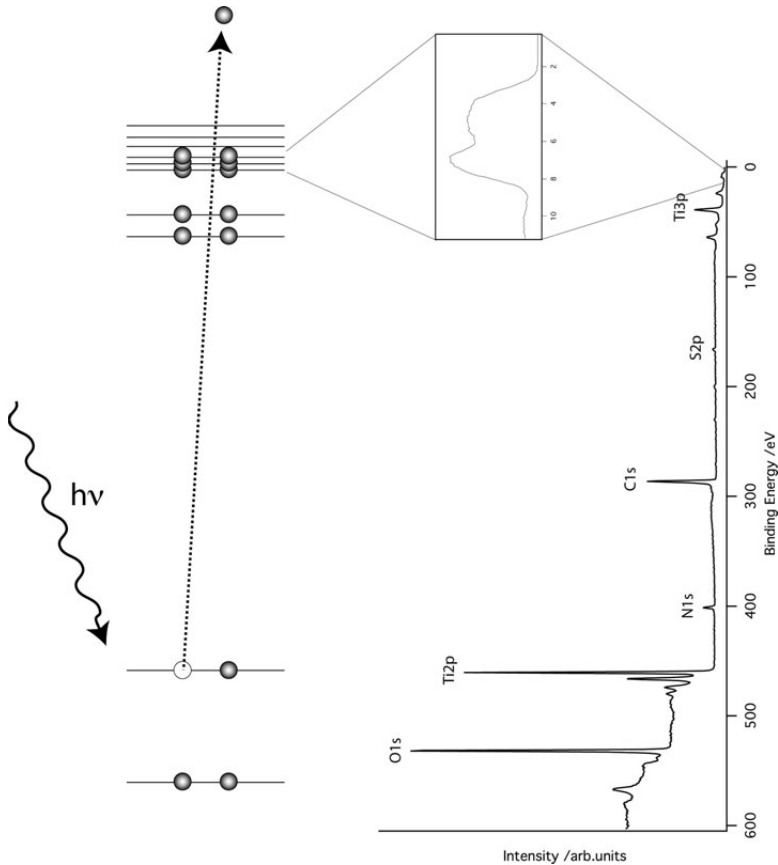


Figure 5. A schematic drawing of photoelectron spectroscopy process.

Each element has a set of unique electron binding energy position usually well separated from each other. By measuring the binding energy of the ejected electrons vs. the number of electrons (or intensity) an element can be identified. However, a specific core level of an element can be influenced by chemical bonds of that particular element. This is known as “chemical shift” which can be used to identify the chemical bonds in a sample. The chemical shift is generally much smaller than the core level separations (not counting splitting of a specific core level).

There are several types of photon sources that are used in PES. In the common commercial XPS instruments, photons are generated through the

bombardment of electrons on a target (Al or Mg) resulting in emission of radiation from the target. The X-ray can be monochromated using a quartz crystals resulting in a higher spectra resolution compared to non-monochromated sources.<sup>73</sup> At synchrotron facilities, electrons traveling at close to the speed of light are accelerated in a storage ring resulting in emission of radiation of continuous energy within a set range. The superiority of synchrotron based photoelectron spectroscopy (PES) is that the photon energy can be varied, and consequently the kinetic energy of electrons, resulting in different depth sensitivity of the measurement.

The mean depth from which a photoelectron can travel without losing energy is defined by the “inelastic mean free path” (IMFP). The intensity,  $I$ , of an electron in a material is proportional to:<sup>74</sup>

$$I \propto I_0 \exp\left(\frac{x}{-\lambda \sin \phi}\right) \quad (8)$$

where  $I$  is the intensity of detected photoelectrons,  $I_0$  is the intensity of emitted photoelectron at depth of  $x$  and  $x/\sin\phi$  is the length that  $e^-$  travels in the materials assuming that  $\phi$  is the angles between surface of sample and the electron trajectory direction. The mean free path  $\lambda$  depends to the photoelectron kinetic energy and the sample composition. There have been attempts to define  $\lambda$  for each element as a function of photoelectron kinetic energies, however, for most materials it is rather similar and the so called “universal curve” can be used as an estimation.<sup>75-77</sup>

In this thesis, the surface characterization of electrodes were performed at three different facilities, i) the Swedish synchrotron MAX-IV Laboratory in Lund, ii) In-house commercial XPS, iii) the Helmholtz Centre Berlin (BESSY) synchrotron laboratory in Berlin, Germany.

The PES measurements at the MAX-IV Laboratory were performed using a Scienta R4000 WAL analyzer at beamline I-411 that is equipped with a Zeiss SX-700 plan grating monochromator. A photoelectron kinetic energy of 140 eV was used for all the PES measurements performed in MAX-IV. This implied that the excitation photon energy was changed from 200 to 835 eV depending on the binding energy of the measured core level, thus, resulting in the same depth of analysis for all the elements. The in-house XPS measurements were performed using a PHI 5500 spectrometer with a monochromatized Al  $K\alpha$  radiation (Figure 6). Hard X-ray photoelectron spectroscopy (HAXPES) measurements were performed at KMC-1 beamline at the BESSY storage ring facility in Berlin, Germany. Two excitation energies of 2300 and 6900 eV were used for the HAXPES measurements.

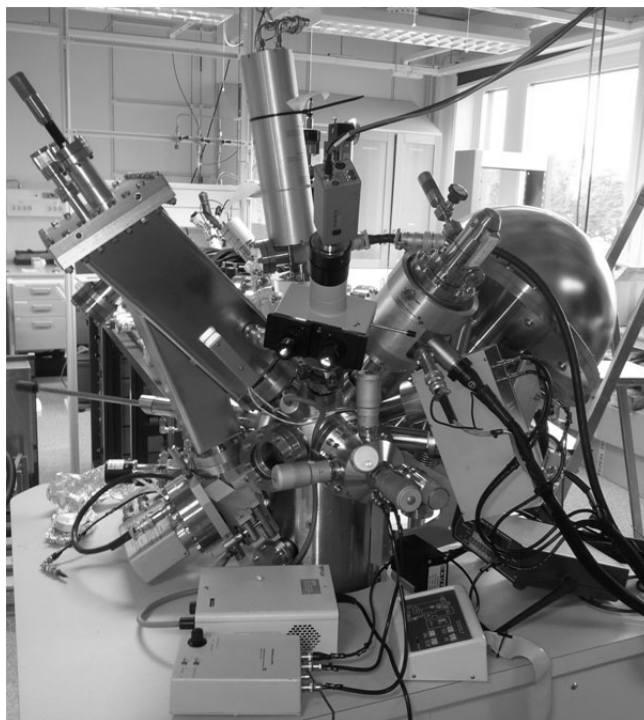


*Figure 6.* A photograph of the in-house XPS instrument.

To analyze cathodes or anodes, batteries were dismantled in an argon-filled glovebox. The samples were then washed with a few drops of DMC. The influence of the washing liquid and the procedure on the sample is still an open question for the experts in the PES battery field. However, it is believed that when an electrode is washed the PES spectra to a higher degree originate from the solid surface of the electrode and limit the information from remaining electrolyte solvents and salts. Moreover, due to the air sensitivity of battery samples, transfer of a sample from the glovebox to a PES analysing chamber was carried out by special designed air-tight transfer units both for the in-house and synchrotron measurements. Generally XPS measurements on battery materials require great care due to the radiation sensitivity of the compound present in a battery, which can cause decomposition during measurements. Also the low pressure inside the chamber can influence the chemistry of surface layers in batteries. Minimizing measurement-time as well as time before measurements is therefore important. For the measurements performed in the synchrotron facilities, samples were transferred in a vacuum-sealed polymer-coated aluminum bag to protect them against contamination by air or moisture. The bag then was opened in an argon-filled glovebox prior to measurements and again transferred to the instrument using a sealed sample exchange cell.

## 4. Summary of Results and Discussion

The results and discussion are divided to four sections. In the first section the results detailing studies on the carbon cathode of the Li-O<sub>2</sub> battery are presented. This is followed by the presentation of results regarding the stability of the electrolyte solvents and salts in the second and third sections, respectively. In the last section, the surface characterization of a lithium anode from a Li-O<sub>2</sub> battery is investigated.

### 4.1. Cathode

In the Li-O<sub>2</sub> battery, ions of lithium and reduced oxygen react to form products in the pores of the cathode. Therefore, the cathode formulation plays a key role to determine the discharge capacity of the cell. Several parameters such as the morphology of carbon in the cathode, the porosity properties of carbon itself, and the carbon loading influence the cathode formulation and consequently the performance of cells.

#### The Effects of Cathode Porosity

Binder is usually one of the necessary components in the assembly of an electrode. This has been commonly the case to produce a porous cathode for a Li-O<sub>2</sub> cell.

It is plausible that the relative amount of binder and its properties have an impact on the porosity properties of the cathode. Although several studies have investigated different parameters influencing the porosity and the discharge capacity of a Li-O<sub>2</sub> cell,<sup>24-30</sup> no systematic study has been devoted to the effect of the amount of binder. To investigate this, different weight ratios of binder to carbon were used to assemble porous cathodes to investigate the influence of the amount of binder on the porosity of the cathode and on the discharge capacity of the cell.

Figure 7 shows the morphology of carbon cathodes with four different weight ratios of Super P carbon to Kynar binder (PVdF-HFP). The micrographs show that the cathodes with lower amounts of binder are most porous since the carbon particles are individually visible. However, the cathodes with higher amounts of binder have a very polymeric surface.

The slurry of each of these catalyst-free cathodes was cast on sheets of glass to produce self-standing electrodes. These self-standing films were analysed in gas adsorption studies to investigate how the surface area and pore volume of the cathode was affected by changing the relative amount of Kynar binder. Figure 8 shows the surface area and pore volume of the cathodes and of a binder-free super P carbon. It is clear that the surface area and pore volume of the cathodes decrease with the increasing amount of Kynar binder. Compared to Super P carbon, addition of even 20 wt% of Kynar reduces the surface area and pore volume by about 30% and 20%, respectively.

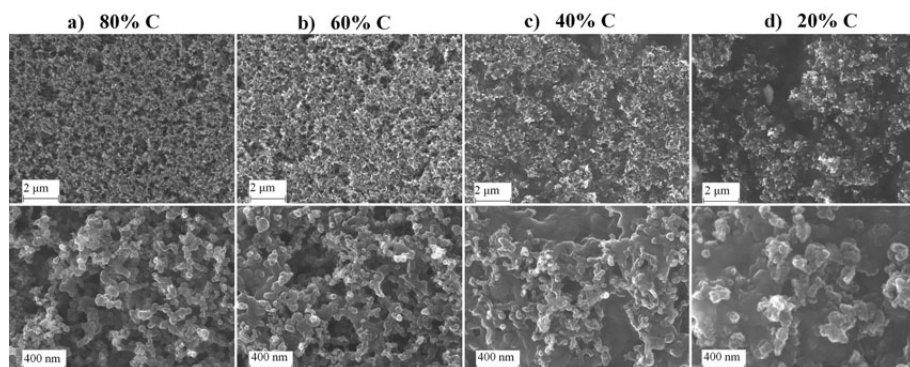


Figure 7. SEM micrographs of cathodes with four different carbon to Kynar ratios at two different magnifications: (a) 80:20, (b) 60:40, (c) 40:60, and (d) 20:80 carbon:Kynar, respectively.

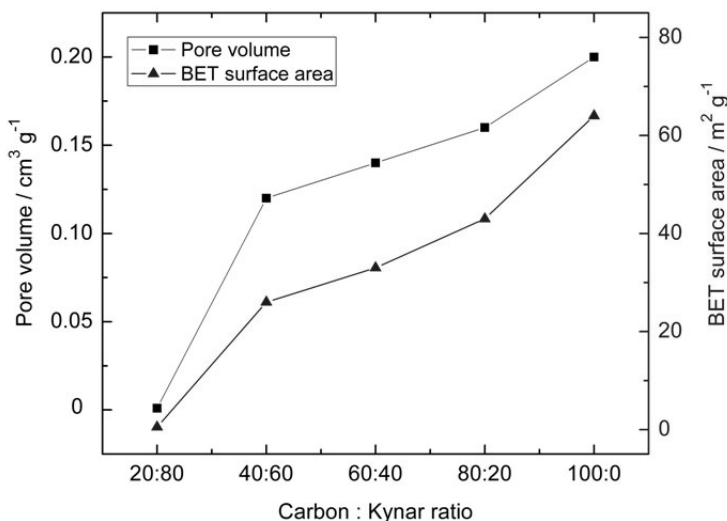


Figure 8. Pore volume and BET surface area of Super P carbon and cathode films with varying ratios of carbon–Kynar.

Figure 9 shows the PSD of Super P and the cathodes with different amounts of Kynar binder. The PSD results indicate that most of the pores smaller than 300 Å are blocked when the amount of Kynar exceeds 40 wt%. It can also be seen that the addition of even 20 wt% of Kynar influences the PSD of Super P carbon.

Therefore, Figures 7-9 clearly show that morphology and porosity properties of carbon cathode are very much dependent to the cathode formulation.

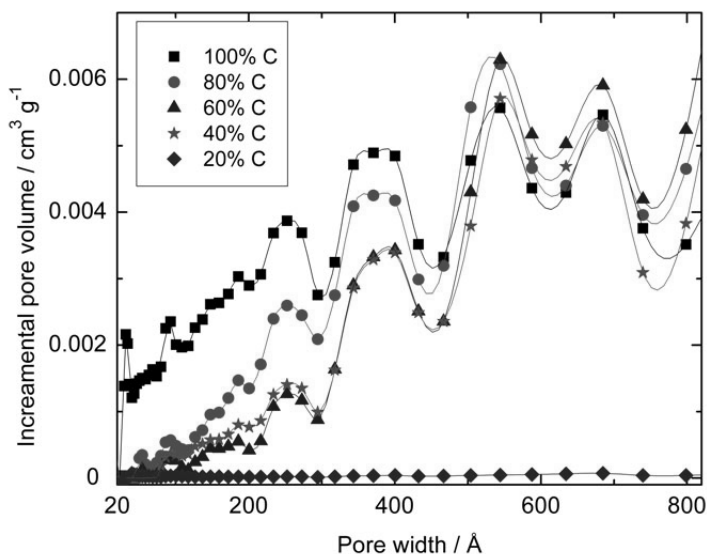


Figure 9. PSD of Super P carbon and the self-standing cathodes with varying the weight ratios of carbon to Kynar.

These electrodes were then tested as a cathode material in Li-O<sub>2</sub> batteries. The changes in the surface area, pore volume and PSD of carbon cathodes significantly influenced the discharge capacities of the Li-O<sub>2</sub> cells as shown in Figure 10. The highest capacities of the first discharge were obtained using the lowest amount of Kynar binder in the cathode, regardless of electrolyte chemistry, confirming that the porosity properties of the cathode influence the discharge capacity of the cell. It is worth mentioning that the chemistry of the solvent also affects the discharge capacity. In general, the use of EC:DEC (2:1) and PC:DEC (1:1) resulted in higher capacities compared to PC. This is related to the properties of these solvents. PC compared to the other solvents possesses higher viscosity and lower ion conductivity.<sup>78,79</sup> The higher viscosity of PC implies that some of the meso- or micropores of the cathode may be inaccessible to molecules of PC.

Further results regarding the influence of the amount of binder on the cell performance are presented **paper I**.



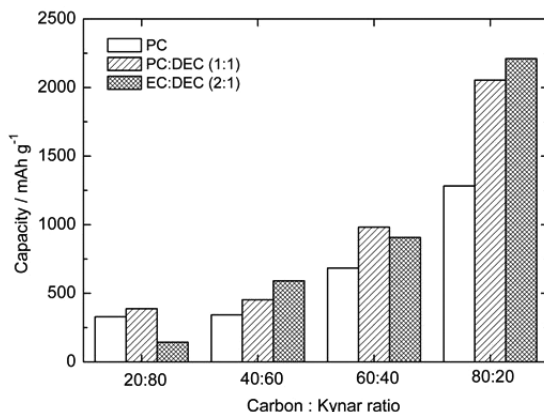


Figure 10. Discharge capacity as a function of the composition of the cathode and the electrolyte.

## Binder Decomposition

During a further study it was found that Kynar binder was unstable in the Li-O<sub>2</sub> battery (**paper II**). In this study Kynar together with Super P carbon and  $\alpha$ -MnO<sub>2</sub> catalyst were used to assemble porous cathodes of Li-O<sub>2</sub> cells which were galvanostatically cycled using ether based electrolytes: 0.5 M LiB(CN)<sub>4</sub> in TEGDME or PEGDME.

The cells were stopped after few cycles at the discharged state and then the cathodes of the cells were analysed using HAXPES. Figure 11 shows the F 1s spectra of these cathodes. For comparison, the F 1s spectra of a reference cathode and two cathodes stored for 2 days in identical cells without applying any current or voltage are also presented in Figure 11. The peak at a binding energy of ~688 eV which is present in the all the spectra represents F within the Kynar binder. The spectra show that a peak at the binding energy of 685 eV, is present in the cycled cathode, but absent in the reference and stored cathodes. This peak reveals the presence of LiF on the surface of carbon cathodes. Since non-fluorinated electrolytes were used in this study, Kynar binder is the only source of F. Therefore, the presence of LiF on the surface of the cycled cathodes indicates that Kynar binder decomposed during the cell cycling to form LiF. The associated results are presented in **paper II**.

The mechanism for this decomposition has been discussed in the literature. It has been proposed that PVdF in contact with LiO<sub>2</sub> undergoes chemical dehydrofluorination to form LiF.<sup>80</sup> Formation of LiF can passivate the surface of the cathode as well as clog the pores resulting in cell failure. It should be noted that the pathway of decomposition may also be linked to the decomposition products of ether based solvents during battery cycling.<sup>38</sup>

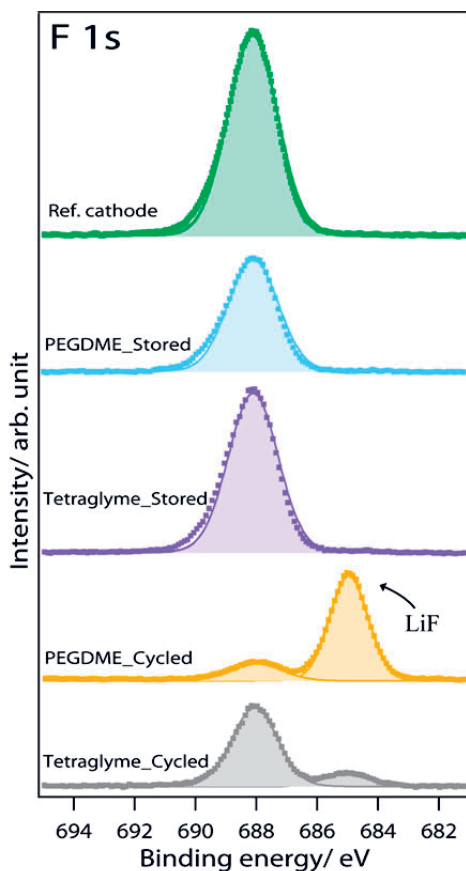


Figure 11. F 1s spectra of the reference, stored and cycled cathodes of Li-O<sub>2</sub> cells using LiB(CN)<sub>4</sub> in PEGDME or Tetraglyme electrolytes. The photon energy was 2300 eV.

### Chemical Stability of Cathode Components

Most of the work in the literature focuses on post mortem analysis of cycled battery systems to assess the stability of the components. However, these results are a mixture of both electrochemical and chemical instability. In an attempt to clarify this confusing system, the chemical stability of cathode components in contact with Li<sub>2</sub>O<sub>2</sub> was investigated (**paper III**). In order to do that, a cathode wetted by electrolyte was kept in contact with Li<sub>2</sub>O<sub>2</sub> powder for 24 h and then it was analysed by XPS. For this study, the most common formulation of cathode used in the literatures in which Kynar binder, α-MnO<sub>2</sub> and Super P carbon are mixed was used. Also two PC and TEGDME based electrolytes were used to wet the cathodes. For comparison, cathodes wetted by electrolyte without being in contact with Li<sub>2</sub>O<sub>2</sub> were also analysed.

Figure 12 shows the F 1s and Mn 2p spectra of these cathodes exposed and not exposed to  $\text{Li}_2\text{O}_2$  using both electrolyte systems. The top spectra belong to a carbon cathode exposed to 0.1 M  $\text{LiClO}_4$  in TEGDME electrolyte for 24 h. The F 1s spectrum contains mainly one peak at 688 eV representing Kynar binder. However, LiF (at 685 eV) could be detected when a cathode was kept in contact with the TEGDME based electrolyte and  $\text{Li}_2\text{O}_2$ . Since the binder was the only source of F, the LiF peak indicates that Kynar binder decomposes in contact with TEGDME based electrolyte and  $\text{Li}_2\text{O}_2$ . Similar results (not presented here) were obtained using DME instead of TEGDME. However, when a similar experiment was performed using a PC electrolyte instead of an ether based system only traces of LiF were observed on the surface (see the two bottom spectra in F 1s and Mn 2p spectra in Figure 12). This suggests the Kynar binder is stable in contact with PC and  $\text{Li}_2\text{O}_2$ .

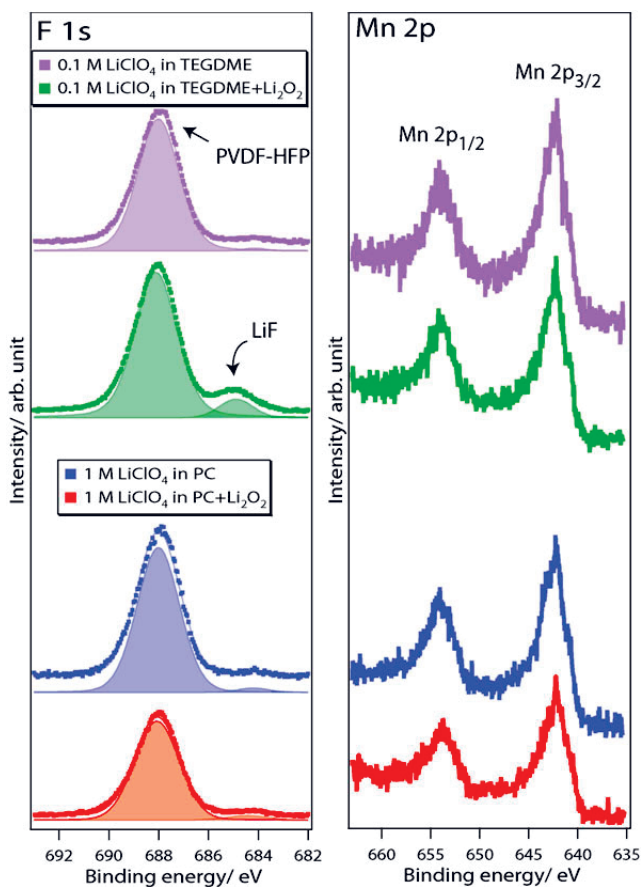
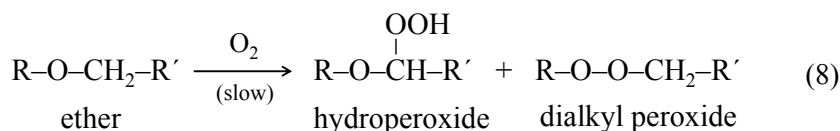


Figure 12. F 1s and Mn 2p spectra of cathodes after being exposed to TEGDME electrolyte (purple spectra), TEGDME electrolyte +  $\text{Li}_2\text{O}_2$  (green spectra), PC electrolyte (blue spectra), and PC electrolyte +  $\text{Li}_2\text{O}_2$  (red spectra). The photon energy was 1487 eV.

In the next section (electrolyte solvent) it will be shown that both TEGDME and PC solvents decompose in contact with  $\text{Li}_2\text{O}_2$ . However, the spectra in Figure 12 showed the decomposition of Kynar solely in the case of TEGDME based sample and not in the case of the PC based sample. Therefore, the results imply that ether based solvents such as TEGDME and DME decompose chemically in contact with  $\text{Li}_2\text{O}_2$  and the decomposition products in turn decompose Kynar binder. However, the decomposition products of carbonate based solvents such as PC are not reactive towards the Kynar binder (**paper III**).

By combining two facts, the decomposition of Kynar by  $\text{Li}_2\text{O}_2$  in an ether based electrolyte can be explained by: i) it is known that ethers in presence oxygen oxidize slowly to form hydroperoxides and/or dialkyl peroxides which are chemically reactive.<sup>81</sup> In this reaction  $\text{O}_2$  decomposes ethers via hydrogen abstraction to hydroperoxide.



ii) It has been suggested that  $\text{Li}_2\text{O}_2$  tends to abstract hydrogen from a carbonate based electrolyte resulting to decomposition of the electrolyte.<sup>37</sup>

Thus, it is anticipated that  $\text{Li}_2\text{O}_2$  similar to  $\text{O}_2$  decomposes ethers by hydrogen abstraction resulting in the formation of hydroperoxide. This chemically reactive compound in turn may decompose Kynar binder.

The results showed no noticeable changes in  $\alpha\text{-MnO}_2$  indicating that this catalyst is chemically stable in contact with  $\text{Li}_2\text{O}_2$ .

## Summary of Studies on Cathode

- The relative amount of binder influences the surface, pore size distribution and pore volume of the porous carbon cathode.
- Increasing the relative amount of Kynar decreases the discharge capacity of the  $\text{Li-O}_2$  battery; as a consequence of the decrease in the surface area and pore volume in the cathode.
- Kynar binder decomposes in a  $\text{Li-O}_2$  cell with ether electrolytes.
- Degradation of ether electrolyte by  $\text{Li}_2\text{O}_2$  results in the decomposition of Kynar binder.

## 4.2. Electrolyte Solvent

As mentioned in the Chapter 2, one of the most difficult challenges for the Li-O<sub>2</sub> battery is still finding a stable electrolyte. This is now well understood since several publications have recently been devoted to the mechanism of the electrolyte decomposition.

This PhD study started by using carbonate based electrolytes since they were the most commonly used electrolyte for Li-O<sub>2</sub> cells. The promising results published by Bruce *et al.* in 2006 to 2008 were based on using PC, a member of the family of carbonate based solvents.<sup>12-14</sup> Therefore, in this work, the reaction products in Li-O<sub>2</sub> cells using PC or EC/DEC based electrolytes were investigated. The results regarding these studies are presented in **papers IV** and **V**.

### The Cycling Performance of Carbonate Electrolytes

Initially cells were constructed using a 1 M LiPF<sub>6</sub> in PC or EC/DEC electrolytes, however, rapid capacity fading was seen in both cases. Typically 3-10 cycles above 1000 mAh/g (calculated based on the amount of carbon in the cathode) was followed by a dramatic decrease in the discharge capacity. Figure 13 shows two examples of the Li-O<sub>2</sub> cells with PC or EC/DEC based electrolytes.

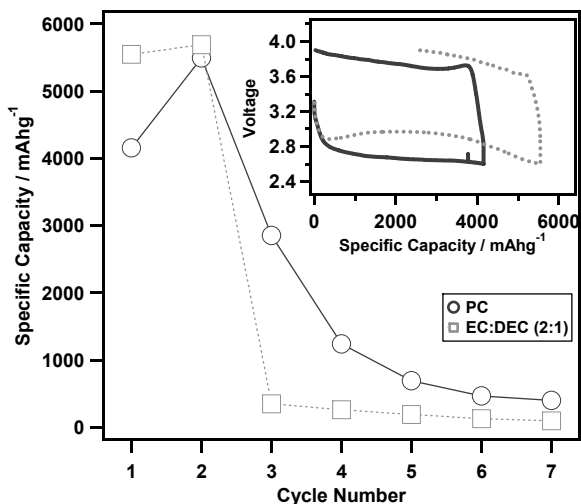
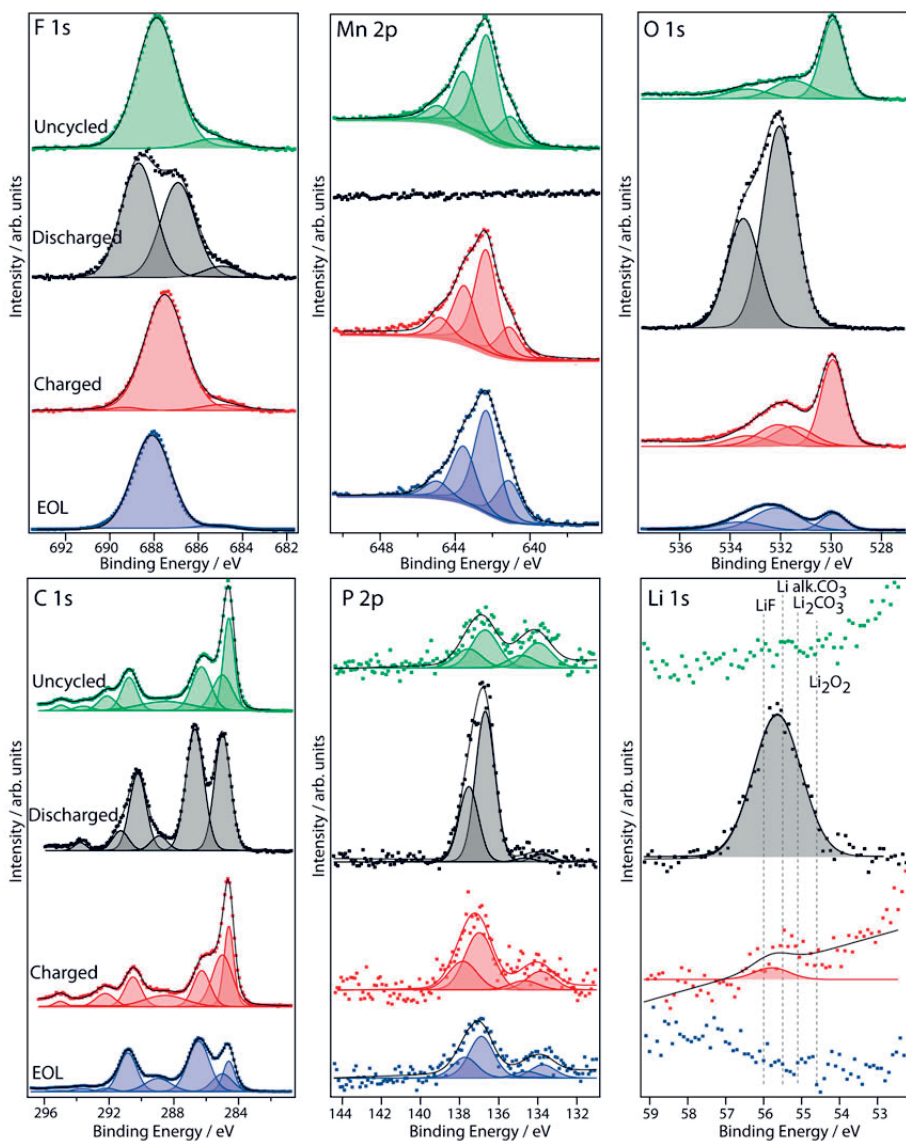


Figure 13. Capacity fading of Li-O<sub>2</sub> cells with  $\alpha$ -MnO<sub>2</sub> nanowire catalyst containing 1 M LiPF<sub>6</sub> in PC or EC:DEC (2:1) at current density of 70 mA/g of carbon with lower and higher cutoff voltages of 2.6 and 3.9 V, respectively. Inset: Voltage as a function of capacity for the first discharge/charge cycle.

In order to determine the reaction products formed in discharging and charging XPS was used for the surface characterization of the cathode from disassembled cells. Figure 14 shows the F 1s, Mn 2p, O 1s, C 1s, P 2p, and

Li 1s spectra of the carbon cathodes removed from Li-O<sub>2</sub> cells at discharge, charged and end of life (EOL) states using 1 M LiPF<sub>6</sub> in PC electrolyte.



**Figure 14.** F 1s, Mn 2p, O 1s, C 1s, P 2p, and Li 1s spectra of the carbon cathodes of the Li-O<sub>2</sub> cells at the uncycled, discharged, charged, and EOL states using 1 M LiPF<sub>6</sub> in PC electrolyte. The uncycled, discharged, and charged samples were measured using an in-house XPS with a photon energy of 1487 eV while the EOL sample was measured using HAXPES with a photon energy of 2300 eV.

The XPS spectra of the cells showed the presence of no Li<sub>2</sub>O<sub>2</sub> or Li<sub>2</sub>O on the carbon cathode after discharging the cell (since the Li<sub>2</sub>O<sub>2</sub> peak, which

would appear at binding energies of 531.5 and 54.6 eV in the O 1s and Li 1s spectra, respectively, are absent).<sup>33</sup> However, the results revealed that PC decomposes to carbon-based species such as  $C_3H_6(OCO_2Li)_2$ ,  $Li_2CO_3$ , and  $CH_3CO_2Li$  during the discharge. This is in agreement with results indicating decomposition of PC obtained using XPS<sup>40,82,83</sup>, FTIR<sup>31,32,83</sup>, XRD<sup>31,35,82</sup>, NMR<sup>31,82</sup>, Raman, and mass spectroscopy.<sup>31,35,82</sup> Furthermore, computational studies also indicated that PC is not stable in the Li-O<sub>2</sub> battery and suggest that decomposition to carbonate based species is expected.<sup>36,84</sup>

The absence of MnO<sub>2</sub> peaks in the Mn 2p and O 1s spectra of the discharged sample shown in Figure 14 indicates that a layer of discharge reaction products is formed on the cathode surface after discharging. Since the XPS spectra in Figure 14 were obtained by using a photon energy of 1487 eV, the absence of MnO<sub>2</sub> peaks reveals that the formed surface layer is thicker than 5 nm.<sup>76,85</sup> However, peaks from MnO<sub>2</sub> are seen in the Mn 2p spectrum of the discharged sample when using HAXPES with a photon energy of 2300 eV (**paper IV**). Since the higher energy photons will penetrate further through the surface layers (discussed in the experimental section) when these result are considered together we can conclude that the decomposition of PC during the discharge results in the formation of a 5–10 nm thick layer on the carbon cathode. This layer is built up predominantly of C and O, being approximately 70% of the surface atomic percentage. The XPS results in Figure 14 also show that the formed surface layer is removed from the cathode during the charging of the cell because the MnO<sub>2</sub> peaks are revealed in the Mn 2p and O 1s spectra of the charged sample. This is in agreement with the mass spectroscopy studies<sup>31,82</sup> which indicate that products formed due to the decomposition of PC degrade to CO<sub>2</sub> gas during the charging of the cell. Figure 15 shows a schematic drawing of the surface layer formed and removed during discharging and charging, respectively, of the Li-O<sub>2</sub> battery with a carbonate based electrolyte.

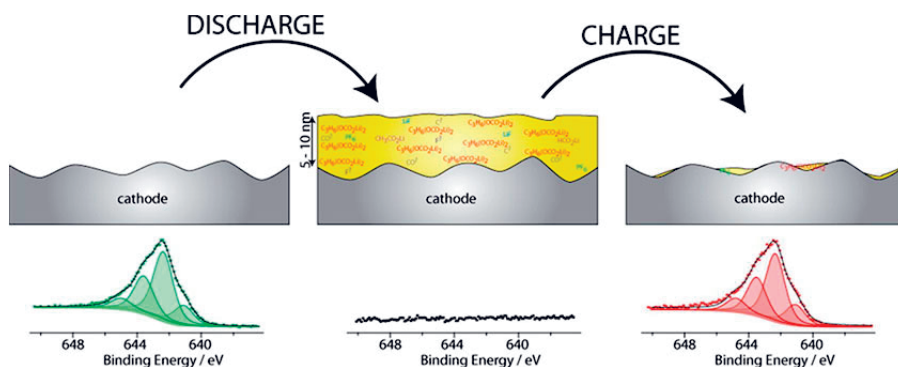
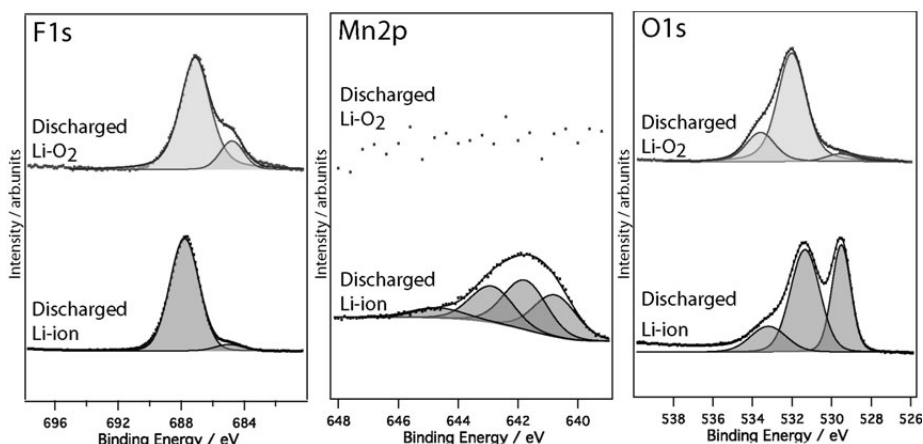


Figure 15. A schematic drawing of the cathode surface of the Li-O<sub>2</sub> battery with carbonate based electrolytes and representative Mn 2p XPS spectra.

Furthermore, we compared the performance of another common carbonate based solvent, EC/DEC, to that of PC. The results suggested that compared to PC, EC/DEC is slightly more stable (**paper V**). However, EC/DEC based electrolytes also decomposes during the discharge forming a surface layer on the cathode.

To evaluate the influence of oxygen on the decomposition of these carbonate based electrolytes, identical batteries were also assembled in the absence of oxygen. The non-oxygen cell is basically a Li-ion battery (some lithium intercalation is expected in the  $\text{MnO}_2$  catalyst) which is expected to show no, or minor, electrolyte decomposition on the cathode. Figure 16 shows the XPS spectra of the cathodes of the cells discharged in the presence and absence of oxygen using 1 M  $\text{LiPF}_6$  in EC/DEC (2:1) electrolyte. The absence of  $\text{MnO}_2$  peaks in the Mn 2p spectrum of the discharged Li- $\text{O}_2$  cathode indicates that a surface layer formed on the cathode is due to the decomposition of the solvent, as explained above. This surface layer has a thickness  $\sim 5$  nm since the  $\text{MnO}_2$  peak is slightly visible in the O 1s spectrum of the discharged Li- $\text{O}_2$  cathode. However, such a layer did not form on the cathode of the non-oxygen cell. In addition, the F 1s spectra display that LiF is formed on the cathode surface of the oxygen cell. However, LiF formation was minor in the non-oxygen cell. When we consider these results together it indicates that the formation of LiF is due to the decomposition of  $\text{LiPF}_6$  salt or Kynar binder and only occurs in the oxygen cell.

It has been suggested that the decomposition of carbonate based electrolytes takes place due to a nucleophilic attack, proton/hydrogen abstraction, or electron transfer by a super oxide ion or by  $\text{Li}_2\text{O}_2$ .<sup>31,34–36,39</sup>



**Figure 16.** F 1s, Mn 2p, and O 1s spectra of cathodes of Li- $\text{O}_2$  and identical Li-ion cells (in the presence and absence of oxygen) at the discharged and charged state compared with the spectra of a pristine cathode. The photon energy was 1487 eV.



## Chemical Decomposition of Carbonate Solvents by $\text{Li}_2\text{O}_2$

Beside the role of the super oxide radical in the decomposition of the electrolyte solvents,  $\text{Li}_2\text{O}_2$  as the final discharge product of the cell may also react chemically with electrolytes. However, the chemical reactivity of the  $\text{Li}_2\text{O}_2$  has been neglected until very recently.<sup>37,51-53</sup>  $\text{Li}_2\text{O}_2$ , similar to other alkali metal peroxides, is a very strong oxidizing agent<sup>86</sup> and thus its plausible reaction with cell components such as electrolyte solvents and salts needs to be considered.

Therefore, the chemical stability of carbonate based electrolyte toward  $\text{Li}_2\text{O}_2$  was studied using XPS (**paper III**). For this study, only  $\text{Li}_2\text{O}_2$  powder was used with no binder, carbon or catalyst. In this design, layers of  $\text{Li}_2\text{O}_2$  powder was placed on an aluminum substrate and exposed to an electrolyte and then brought to the XPS instrument using an air-tight argon filled transfer module. The studied carbonate based electrolytes are listed in Table 1 and the results regarding the stability of these electrolytes in contact with  $\text{Li}_2\text{O}_2$  are presented in **paper III**.

Table 1. *List of carbonate-based electrolytes and solvent used to study the chemical stability in contact with  $\text{Li}_2\text{O}_2$ .*

Electrolyte solvents and salts
1 M $\text{LiPF}_6$ in PC
1 M $\text{LiPF}_6$ in EC:DEC (2:1)
0.8 M $\text{LiBF}_4$ in EC:DEC (2:1)
0.1 M $\text{LiPF}_6$ in PC
PC solvent / no salt

In this subsection the stability of only 1 M  $\text{LiPF}_6$  in PC or EC/DEC, which are commonly used as an electrolyte for Li- $\text{O}_2$  and Li-ion batteries, are discussed.  $\text{Li}_2\text{O}_2$  samples were exposed to these two electrolytes for 10 min and 48 h and then analysed by XPS. The reason of choosing two exposure times was to compare products formed due to reaction between  $\text{Li}_2\text{O}_2$  and the electrolyte in relatively short and long exposure times. The results from the shorter exposure time, 10 min, suggest how the electrolytes will react as soon as  $\text{Li}_2\text{O}_2$  forms during discharge. The results from the longer exposure time, 48 h, about the length of 1-3 cycles in a Li- $\text{O}_2$  cell, indicate the condition of electrolytes in contact with  $\text{Li}_2\text{O}_2$  after a few cycles.

Figure 17 shows the F 1s, O 1s, C 1s, and P 2p spectra of  $\text{Li}_2\text{O}_2$  samples after being exposed to 1 M  $\text{LiPF}_6$  in PC or EC/DEC electrolytes for 10 min or 48 h. The F 1s and P 2p spectra indicate that  $\text{LiPF}_6$  decomposes in contact with  $\text{Li}_2\text{O}_2$  (this is discussed more in the next section). The peaks at 287 and 289.7 eV in the C 1s spectra represent the ether and carbonate species, respectively. These two peaks originate from decomposed rather than from remaining solvents since i) the samples were washed by DMC before XPS

analysis and ii) the relative amount of these two peaks is different from the relative amount of ether to carbonate bonds in the molecule structure of these solvents. The formation of carbonate species is in agreement with a recent computational study which suggested that  $\text{Li}_2\text{O}_2$  decomposes PC to alkyl carbonates.<sup>37</sup> Figure 18 is a schematic of the proposed reaction mechanism describing the reaction between  $\text{Li}_2\text{O}_2$  and PC or EC/DEC to form lithium alkyl carbonates. PC and EC/DEC are good solvating agents for  $\text{Li}^+$  while not for oxygen anions. As a consequence of this fact, the negatively charged part of the  $\text{Li}_2\text{O}_2$  molecule,  $\text{O}_2^{2-}$ , abstract  $\text{H}^+$  from PC to balance the excess negative charge of  $\text{O}_2^{2-}$ .<sup>37</sup> This further leads to the ring opening of PC or EC,<sup>87,88</sup> and consequently the formation of lithium alkyl carbonates and  $\text{H}_2\text{O}_2$  which have been suggested as the reaction products in the cell.<sup>33,38,80</sup>

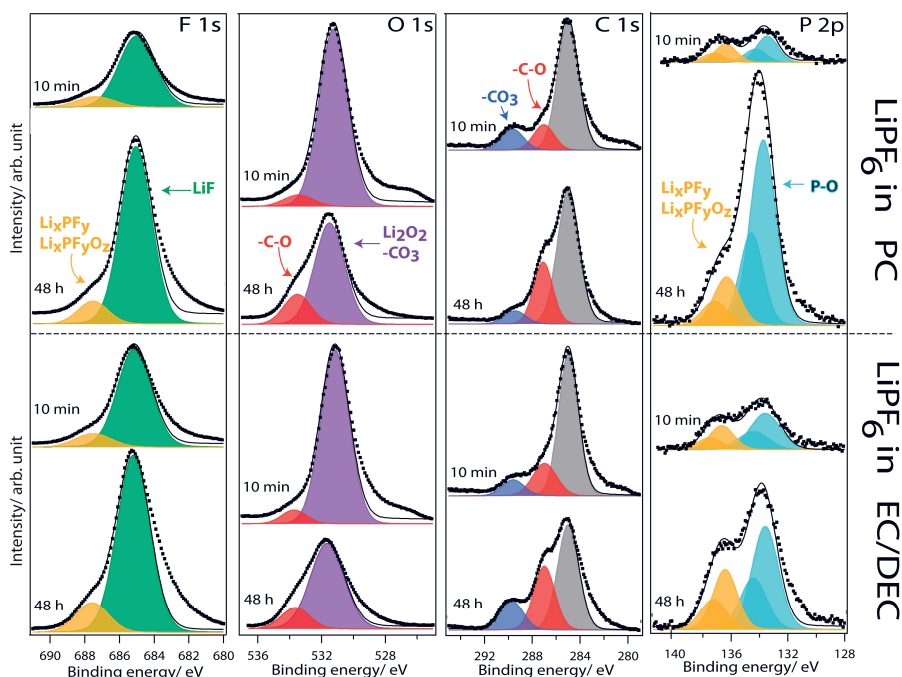


Figure 17. F 1s, O 1s, C 1s, and P 2p spectra of  $\text{Li}_2\text{O}_2$  samples after being exposed to 1 M  $\text{LiPF}_6$  in PC or in EC/DEC electrolytes for short (10 min) or long (48 h) time.

The relative amount of the ether peak at 287 eV in the C 1s spectra increases from short to long exposure times indicating that PC in contact with  $\text{Li}_2\text{O}_2$  also decomposes to ether species. This increase in the ether species is supported by the peak at 533.6 eV in the O 1s spectra. It has been shown that PC decomposes to oligomer chains of poly(ethylene oxide)  $(\text{CH}_2\text{CH}_2\text{O})_n$  (PEO) and/or ROLi due to reaction with  $\text{PF}_5$  formed due to the decomposition of  $\text{LiPF}_6$ .<sup>89</sup>  $\text{Li}_2\text{O}_2$ , similar to  $\text{PF}_5$ , is a strong oxidizing agent and thus its reaction with PC or EC/DEC solvents may explain the formation of ether

species. The increase in the relative amount of the ether peak is larger for the PC sample than that for the EC/DEC sample. This suggests that compared to PC, EC/DEC is more stable in contact with  $\text{Li}_2\text{O}_2$ . To validate these results, similar experiments were performed using  $\text{LiBF}_4$  in EC/DEC electrolyte. The XPS results of that experiment also indicated that the decomposition of EC/DEC solvent to ether species occur to a smaller extent compared to that in the PC solvent. This is in line with conclusion made in **paper III** where the XPS analysis of the cathodes of PC and EC/DEC cells revealed that PC, compared to EC/DEC, decomposes to a larger extent.

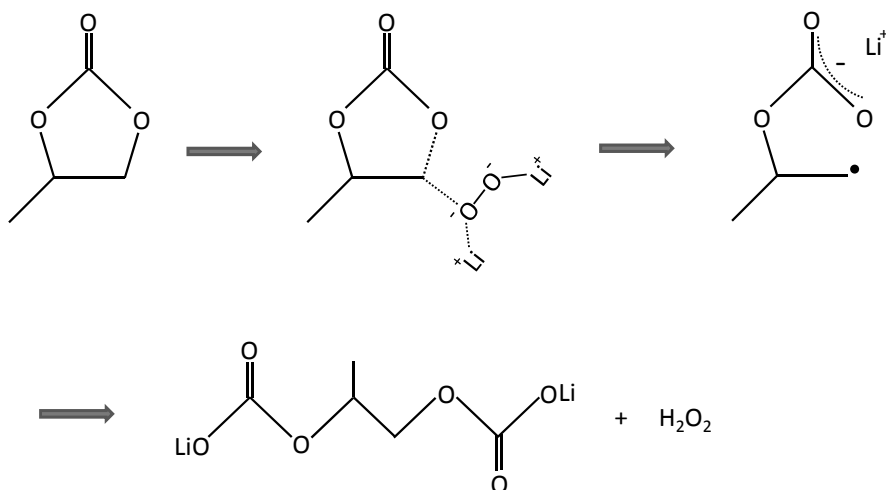


Figure 18. A schematic of proposed reaction mechanism between  $\text{Li}_2\text{O}_2$  and PC or EC/DEC.

Compared to PC, a mixture of EC with a linear carbonate solvent such as DEC or DMC has been shown to improve the performance of Li-ion batteries. This has been attributed to the formation of a stable SEI on the negative electrode when using EC mixed with a linear carbonate. However, the origin of this improvement as well as higher stability of EC/DEC compared to PC observed in this study is not clear.

## The Cycling Performance of Ether Electrolytes

As explained in the introduction, as the carbonate based electrolytes were found to be unstable in Li- $\text{O}_2$  batteries, ether based electrolytes were suggested as an alternative. The ether based electrolytes seemed to be promising because it was shown that  $\text{Li}_2\text{O}_2$  forms as a discharge product and this even increased the number of cycles that were reported.<sup>41-45</sup>

Therefore, we investigated the performance of Li- $\text{O}_2$  cells using Tetraglyme and PEGDME solvents (**paper II**). Due to the instability of

LiPF<sub>6</sub> in the Li-O<sub>2</sub> battery<sup>33</sup> and due to poor solubility of LiPF<sub>6</sub> in ether solvents, LiB(CN)<sub>4</sub> was used as the salt. It has been shown that LiB(CN)<sub>4</sub> with high thermal and electrochemical stability can improve the performance of a Li-ion battery.<sup>90</sup>

Figure 19 shows the discharge/charge performance of Li-O<sub>2</sub> cells with these ether based electrolytes displaying a rapid capacity fading from the first to the 7<sup>th</sup> cycle.

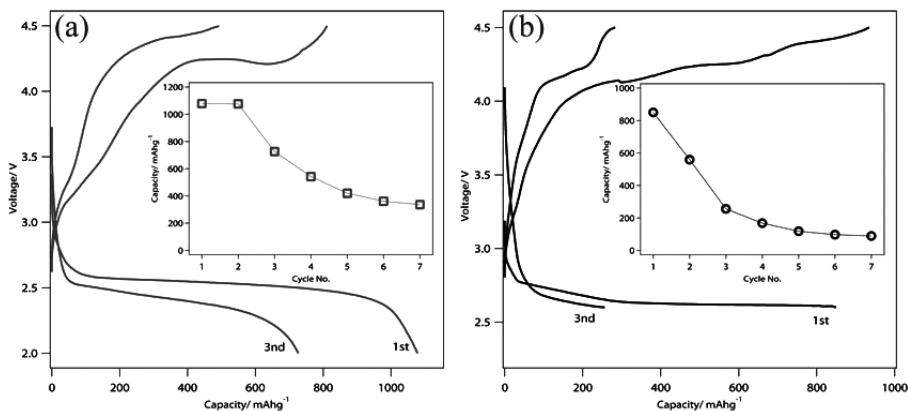


Figure 19. Voltage of first and third discharge/charge plateaus of cells with LiB(CN)<sub>4</sub> in PEGDME (a) and Tetraglyme (b) electrolytes, at a current density of 70 mA/g of carbon, respectively. Inset: Discharge capacities vs. cycle number.

To characterize the reaction products the carbon cathodes of the cells at the discharged state were analyzed using HAXPES. Figure 20 shows the Mn 2p, O 1s, and C 1s spectra of the cathodes. The peaks at 642.3 and 654 eV in the Mn 2p spectrum and the peak at 529.9 eV in the O 1s spectrum of the reference cathode represent MnO<sub>2</sub> catalyst used in the assembly of the cathode. The absence of these peaks in the Mn 2p and O 1s spectra of the PEGDME cell implies that a thick layer formed on the surface of the cathode. However, for the cathode removed from the Tetraglyme cell, these peaks are visible although their intensities are smaller compared to the intensity of the reference cathode. The surface layer is made of LiF formed due to decomposition of Kynar binder (see section 3.1) and of decomposition products of the solvents. The relatively high intensity of the peak at 286.6 eV in the C 1s spectra of the cycled cathodes indicates the presence of ether species originating from decomposition of the solvents.

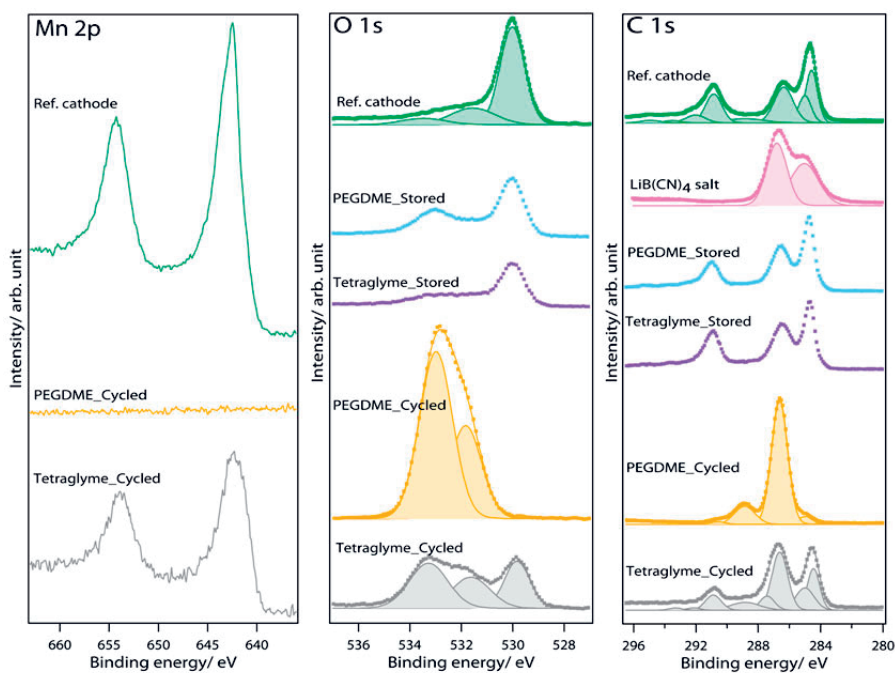


Figure 20. Mn 2p, O 1s, and C 1s spectra of the reference and cycled cathodes using  $\text{LiB}(\text{CN})_4$  in PEGDME or Tetraglyme. The photon energy was 2300 eV.

The reason that ether based electrolytes have recently become popular in the  $\text{Li-O}_2$  battery research is that  $\text{Li}_2\text{O}_2$  can be formed as the discharge product of the cell. This has been proved using analytical techniques such as XRD, Raman, etc.<sup>22,43–45</sup> However, the formation of  $\text{Li}_2\text{O}_2$  and the ability to cycle the cells do not necessarily prove that the cell is truly reversible. Using XPS as a surface sensitive technique which can detect crystalline as well as amorphous reaction products, it has been shown that ether based electrolytes are not stable in the  $\text{Li-O}_2$  battery.<sup>46,48</sup> This is in line with mass spectroscopy results indicating the formation of  $\text{CO}_2$  due to the decomposition of an ether based electrolyte.<sup>47</sup>

Indeed, ether electrolytes are weak candidates for the  $\text{Li-O}_2$  battery since it has been shown that the  $\text{O}_2$  molecule can oxidize ethers via a process called “autooxidation” (see Eq. 8), this proceeds by abstracting a hydrogen from ethers to produce hydroperoxides.<sup>81,91</sup>

### Chemical Decomposition of Ether Solvents by $\text{Li}_2\text{O}_2$

Furthermore, as with any electrolyte ethers need to be stable in contact with  $\text{Li}_2\text{O}_2$ . Thus, we investigated the stability of an ether based electrolyte toward  $\text{Li}_2\text{O}_2$  similar to the experiment we performed for the carbonate based electrolytes (**paper III**).

Figure 21 shows the O 1s and C 1s spectra of the  $\text{Li}_2\text{O}_2$  sample after being exposed to 0.1 M  $\text{LiClO}_4$  in TEGDME. The peak at 289 eV with a relatively high intensity in the C 1s spectrum indicates the presence of carboxylate species on the surface of  $\text{Li}_2\text{O}_2$  sample. The peak at 532.1 eV in the O 1s spectrum confirms the presence of carboxylates on the surface of  $\text{Li}_2\text{O}_2$ . These carboxylate species can be assigned to hydroperoxides which contain a carboxylate bond ( $-\text{COO}$ ). Therefore,  $\text{Li}_2\text{O}_2$  via hydrogen abstraction can decompose the TEGDME solvent.

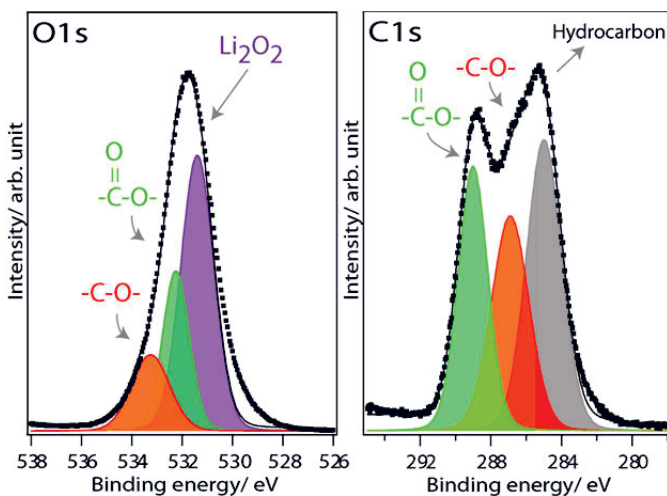


Figure 21. O 1s and C 1s spectra of a  $\text{Li}_2\text{O}_2$  sample after being in contact with 0.1 M  $\text{LiClO}_4$  in TEGDME electrolyte for 48 h.

## Summary of Studies on Electrolyte Solvents

- Carbonate based solvents such as PC or EC/DEC decompose during the discharge of Li- $\text{O}_2$  batteries due to the reaction with the reduced oxygen ions or due to the reaction with  $\text{Li}_2\text{O}_2$ .
- The decomposition of PC or EC/DEC results in the formation of a surface layer between  $\sim 5$  to 10 nm thick which passivates the surface of cathode and of  $\text{MnO}_2$  catalyst.
- Ether solvents such as TEGDME and PEGDME also degrade during the cell cycling due to reaction with  $\text{O}_2$  atmosphere or with reduced oxygen species.
- All the carbonate and ether solvents tested (PC, EC/DEC, TEGDME) were unstable in contact with  $\text{Li}_2\text{O}_2$ .

## 4.3. Electrolyte salt

The stability of Li salt in the Li-O<sub>2</sub> battery is also questionable. Two types of experimental methods were used here to investigate the stability of several common lithium battery salts: i) the stability of a salt during the cell cycling, or ii) chemical stability of a salt in contact with Li<sub>2</sub>O<sub>2</sub>.

### 4.3.1. Stability of Li Salts during Cell Cycling

In an ideal battery a Li salt acts as a charge carrier and is stable to both the electrochemical window of test and chemically to all the components within the battery (excluding the partial decomposition of salts to form the SEI on the anode). The same performance from the salt is also expected in the Li-O<sub>2</sub> battery.

#### **Lithium Hexfluorophosphate (LiPF<sub>6</sub>)**

LiPF<sub>6</sub> as the most common lithium salt was first used in this work to prepare electrolytes. However, the surface characterization of cell cathodes revealed that LiPF<sub>6</sub> salt decomposes during cycling (**paper IV**). The F 1s and P 2p spectra in Figure 14 (see section 4.2) indicate that LiPF<sub>6</sub> decomposes partially to LiF and P-O bond-containing compounds during the cell cycling. This is in agreement with another XPS study indicating that LiPF<sub>6</sub> salt decomposes in the Li-O<sub>2</sub> battery.<sup>49</sup>

#### **Lithium Bis(oxalate)borate (LiBOB)**

LiBOB salt which is known as an alternative non-fluorinated salt to LiPF<sub>6</sub> was also utilized to prepare electrolytes. However, it was observed that the LiBOB salt dissolved in PC decomposes during the cell cycling (**paper V**). The B 1s spectrum in Figure 22 consists of two peaks at 192.9 and 202.8 eV, indicating the presence of B atoms in two environments. The peak at the lower binding energy represents the remaining LiBOB salt. However, the peak at the higher binding energy indicates that B atoms are bound to highly electronegative atoms such as -CF<sub>3</sub> and consequently that LiBOB degraded. Similar results have been reported in the literature regarding the stability of the LiBOB salt.<sup>49-51</sup>

#### **Lithium Perchlorate (LiClO<sub>4</sub>)**

LiClO<sub>4</sub> has been suggested as a possible stable salt for Li-O<sub>2</sub> cells.<sup>49,51</sup> Hence, the stability of LiClO<sub>4</sub> salt was also investigated in this study (**paper V**).

Figure 23 shows the Cl 2p spectra of cathodes of Li-O<sub>2</sub> cells cycled using 1 M LiClO<sub>4</sub> in PC or EC/DEC electrolytes. The Cl 2p spectra are deconvoluted using spin-orbit split doublets for each chemical state (Cl 2p<sub>3/2</sub> and

Cl  $2p_{1/2}$ ) with intensity ratios 2:1 and a peak split of 1.6 eV. The spectrum of the EC/DEC sample consist of one peak at 208.6 eV representing the  $\text{LiClO}_4$  salt; no  $\text{LiClO}_4$  decomposition was observed for this sample. The presence of remaining salt on the surface of the electrodes is not necessarily a proof of salt decomposition. In the case of Li-ion cells it has also been observed that a fraction of salt may remain on the electrode surface even when the electrodes were washed with DMC before XPS analysis.

However, the Cl  $2p$  spectrum of the PC samples consists of two peaks at 198.5 and 208.4 eV. The peak at the lower binding energy represents LiCl and reveals that  $\text{LiClO}_4$  decomposed during the cell cycling using a PC based electrolyte.<sup>92</sup>

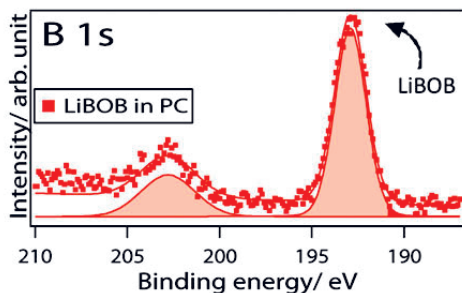


Figure 22. B 1s spectrum of the cathode of a Li-O<sub>2</sub> cell at the charged states using 1 M LiBOB in PC electrolyte. The photon energy was 140 eV.

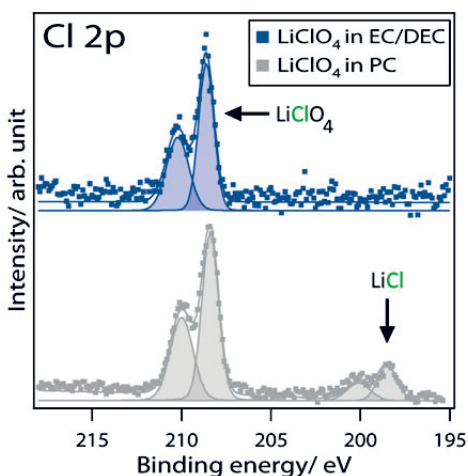


Figure 23. Cl  $2p$  spectra of the cathodes of Li-O<sub>2</sub> cells at the charged state using 1 M  $\text{LiClO}_4$  in PC or EC/DEC electrolytes. The photon energy was 140 eV.



### LiBison (LiB(CN)<sub>4</sub>)

For the sake of achieving a stable salt for the Li-O<sub>2</sub> battery, the stability of LiB(CN)<sub>4</sub> salt was investigated (**paper II**). This salt has been shown to improve the performance of a Li-ion battery<sup>90</sup>, during the cell cycling.

Figure 24 shows the N 1s and B 1s spectra of the LiB(CN)<sub>4</sub> salt and of the stored and cycled cathodes of Li-O<sub>2</sub> cells with 0.5 M LiB(CN)<sub>4</sub> in PEGDME or TEGDME electrolytes. The N 1s spectra of stored and cycled cathode show one peak at 400.1 eV representing remaining LiB(CN)<sub>4</sub> salt on the cathodes surface. The B 1s spectra of cycled cathodes consist of two peaks representing different types of B bonds. The peak at 191.8 eV, visible in the spectra of cycled cathodes matches to the B 1s peak of the salt. However, the cathodes of both PEGDME and TEGDME cells show one additional peak located at the binding energies of 190.1 and 192.7 eV, respectively. The presence of these peaks imply that B atoms formed new bonds due to degradation of LiB(CN)<sub>4</sub> salt. In the case of the TEGDME cell, the additional peak at 192.7 eV indicates that B atoms are bonded to more electronegative atoms compared to C atoms. The peak, thus, can be assigned to the B-F or B-O bonds. The peak at 190.1 eV suggests that B atoms are bonded to less electronegative atoms compared to C atoms.

Overall, the XPS characterization of cathodes removed from cells containing LiB(CN)<sub>4</sub> salt indicated that this salt also decomposes during the cell cycling.

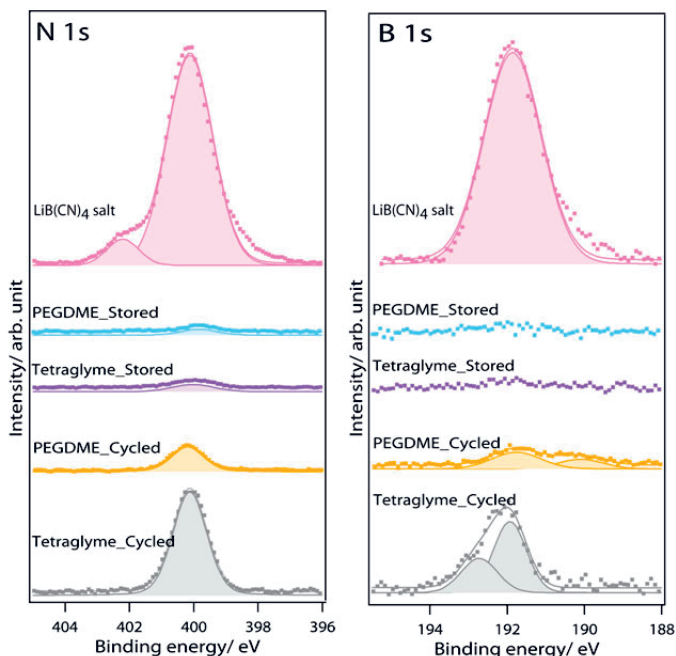


Figure 24. N 1s and B 1s spectra of carbon cathode of Li-O<sub>2</sub> cells cycled using 0.5 M LiB(CN)<sub>4</sub> in TEGDME or PEGDME. The photon energy was 2300 eV.

### 4.3.2. Stability of Li Salts in Contact with $\text{Li}_2\text{O}_2$

After observing the level of breakdown of salts during electrochemical tests, a fundamental study was performed to investigate the stability of Li salts in contact with  $\text{Li}_2\text{O}_2$ . As explained in section 3.2, to study the electrolyte stability  $\text{Li}_2\text{O}_2$  powder was placed on an aluminium plate and exposed to the electrolyte. Using this type of experiment, the stability of several common lithium salts including  $\text{LiPF}_6$ ,  $\text{LiBF}_4$  and  $\text{LiClO}_4$  were investigated (**paper III**).

#### **Lithium Hexfluorophosphate ( $\text{LiPF}_6$ )**

As it is shown in Figure 17, the F 1s spectra of  $\text{Li}_2\text{O}_2$  surfaces indicate that the  $\text{LiPF}_6$  salt decomposes in contact with  $\text{Li}_2\text{O}_2$  to form LiF and  $\text{Li}_x\text{PF}_y/\text{Li}_x\text{PF}_y\text{O}_z$ . This is confirmed in the P 2p spectra in Figure 17. The P-O peak originated from the salt degradation clearly reveals that  $\text{LiPF}_6$  is unstable when exposed to  $\text{Li}_2\text{O}_2$ . The relative intensity of LiF and P-O peaks in the F 1s and P 2p spectra, respectively, increases by increasing the exposure time. This implies that a larger amount of decomposition products from the  $\text{LiPF}_6$  salt form on the surface of  $\text{Li}_2\text{O}_2$  with increasing exposure time indicating that a stable passivation layer is not possible.

#### **Lithium Tetrafluoroborate ( $\text{LiBF}_4$ )**

$\text{LiBF}_4$  is another common lithium salt which has recently been suggested to be stable toward  $\text{Li}_2\text{O}_2$ .<sup>53</sup> Thus, its stability was tested in contact with  $\text{Li}_2\text{O}_2$  using the experimental design explained above.

Figure 25 shows the F 1s and B 1s spectra of  $\text{Li}_2\text{O}_2$  powder after being in contact with 0.8 M  $\text{LiBF}_4$  in EC:DEC (2:1) for 10 min or 48 h. The F 1s spectra consist of two peaks at 685 and 687.2 eV representing LiF and  $\text{LiBF}_4/\text{Li}_x\text{BF}_y\text{O}_z$ . The LiF peak indicates that  $\text{LiBF}_4$  is unstable in contact with  $\text{Li}_2\text{O}_2$  and decomposes to form LiF. The B 1s spectra support this finding. The peak at lower binding energy represents B-O bond containing compounds and indicates that  $\text{LiBF}_4$  salt is degraded. The relative surface compositions of  $\text{Li}_2\text{O}_2$  surfaces after exposure to the  $\text{LiBF}_4$  based electrolytes and the assigned compounds of F, P and C elements are presented in Figure 26a and 26b. The relative amounts of both F and B increase by increasing the exposure time while the relative amount of O decreases. The relative amount of LiF increases from about 4 to 26 at% between 10 min and 48 h exposure times, respectively. This indicates that more  $\text{LiBF}_4$  salt decomposes on the  $\text{Li}_2\text{O}_2$  electrodes from shorter to longer exposure times, similar to that which was observed in the  $\text{LiPF}_6$  based samples.

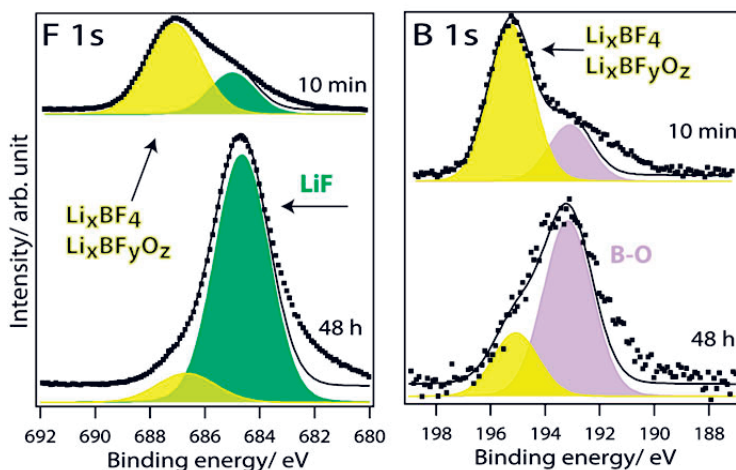


Figure 25. F 1s and B 1s spectra of  $\text{Li}_2\text{O}_2$  after being in contact with 0.8 M  $\text{LiBF}_4$  in EC:DEC (2:1) electrolyte for short (10 min) or long (48 h) time.

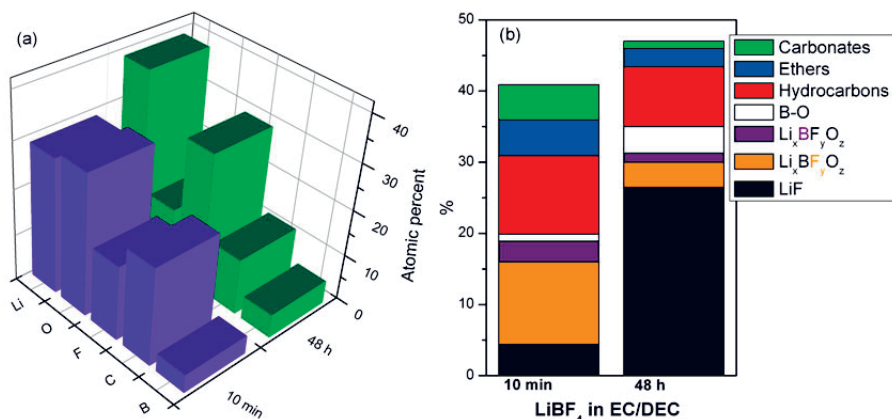
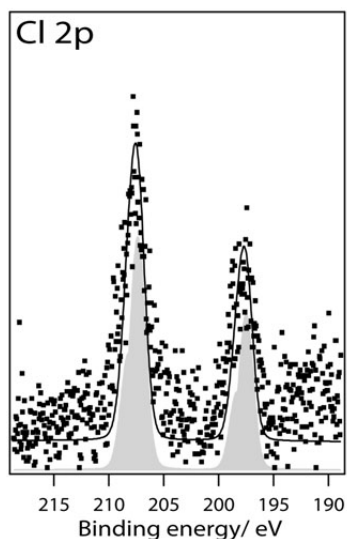


Figure 26. (a) The relative element surface composition of  $\text{Li}_2\text{O}_2$  samples after being exposed to 0.8 M  $\text{LiBF}_4$  in EC:DEC (2:1) electrolyte for 10 min or 48 h. (b) The assigned compounds to the B, F, and C elements and their relative amounts.

### Lithium Perchlorate ( $\text{LiClO}_4$ )

Finally, the stability of the  $\text{LiClO}_4$  salt was also tested in the same way. Surface characterization of  $\text{Li}_2\text{O}_2$  powder exposed to  $\text{LiClO}_4$  containing electrolyte indicates that  $\text{LiClO}_4$  decomposed and formed  $\text{LiCl}$  (Figure 27). It should, however, be noted that  $\text{LiClO}_4$  was dissolved in TEGDME solvent, which is shown to be decomposed in contact with  $\text{Li}_2\text{O}_2$  to form hydroperoxides. Hence,  $\text{LiClO}_4$  may decompose via reaction with decomposition products of TEGDME and not directly by  $\text{Li}_2\text{O}_2$ . This could be further checked by using  $\text{LiClO}_4$  in relatively stable solvents.



*Figure 27.* Cl 2p spectrum of a  $\text{Li}_2\text{O}_2$  sample after being in contact with 0.1 M  $\text{LiClO}_4$  in TEGDME electrolyte for 48h.

## Summary of Studies on Li Salts

- $\text{LiPF}_6$ ,  $\text{LiB}(\text{CN})_4$ , and  $\text{LiBOB}$  salts were found to be unstable during cycling of  $\text{Li-O}_2$  cells.
- $\text{LiClO}_4$  showed no degradation product on the carbon cathode of the cell cycled using  $\text{LiClO}_4$  in EC/DEC. However,  $\text{LiClO}_4$  salt dissolved in PC did decompose to form  $\text{LiCl}$ .
- The decomposition products of the Li salt formed during the cell cycling contributed to the formation of a surface layer on the carbon cathode.
- $\text{LiPF}_6$ ,  $\text{LiBF}_4$  and  $\text{LiClO}_4$  were found to be unstable in contact with  $\text{Li}_2\text{O}_2$  rendering formation of degradation products such as  $\text{LiF}$ ,  $\text{LiCl}$ , and P-O compounds on the surface of  $\text{Li}_2\text{O}_2$ .

## 4.4. Anode

The stability of electrolyte solvents and salts in contact with  $\text{Li-O}_2$  and  $\text{Li}_2\text{O}_2$  have been studied by several researchers, the stability of electrolyte in contact with the lithium anode in the presence of oxygen has, however, not been investigated properly.

Lithium metal has a very negative potential ( $\sim -3$  V vs. SHE) and is very reactive. Therefore, all the nonaqueous solvents in contact with lithium metal decompose partially and form a passivation layer known as an SEI on the lithium metal. The nature of the SEI on lithium metal for Li-ion batteries has been extensively investigated. It has been concluded that many parameters influence the chemistry, morphology, and stability of the SEI making it very complex.<sup>54</sup>

Within this PhD, a study of the SEI formed on the lithium anode of the  $\text{Li-O}_2$  battery was carried out for the first time (to the best of our knowledge) (**paper VI**).<sup>63</sup> This work was initiated as a result of visual observations that a thick black layer forms on the lithium anode after only a few cycles of a  $\text{Li-O}_2$  battery using carbonate based electrolytes (Figure 28). This is unlike the lithium anode of Li-ion batteries cycled using the same electrolyte and current density.

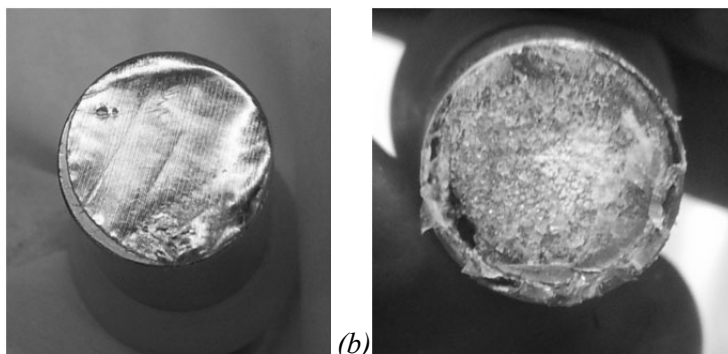


Figure 28. Photograph of pristine (a) and cycled (b) Li anode in a  $\text{Li-O}_2$  cell.

Therefore, to study the SEI on lithium in detail we used XPS to characterize the surface of lithium anode in the  $\text{Li-O}_2$  battery using  $\text{LiPF}_6$  in PC electrolyte. Also, in order to investigate the stability of the SEI, we compared lithium metal removed from cells at the discharged and charged states and a cell stored for two days in oxygen atmosphere.

Table 2 presents the relative surface composition seen for the lithium anode of these cells (assuming a uniform distribution of the elements). The changes in the relative surface composition of the lithium anode from the stored to discharged sample and then from the discharged to charged sample indicate that the SEI is unstable during the cell cycling.

Table 2. *The relative surface composition (at%) of Li anode of the stored, discharged, and charged Li-O<sub>2</sub> cells using 1 M LiPF<sub>6</sub> in PC.*

Element	Stored	Discharged	Charged
C	41	45	50
O	34	22	23
Li	17	13	12
F	7	16	13
P	1	3.3	1.8

Figure 29 shows the XPS core peaks of the elements observed on the surface of lithium anode of the stored, discharged, and charged cells. The details of the peak assignments and the relative amount of the compounds are presented in **paper VI**. In conclusion, LiPF<sub>6</sub> salt and PC solvent both in contact with lithium metal decompose and are involved in the SEI formation. The LiPF<sub>6</sub> salt decomposes to LiF and P-O containing compounds while the PC is degraded to lithium alkyl carbonate, ether, and carboxylate/ester species. Comparing these results with the SEI on Li anode of non-oxygen cells, it can be concluded that the relative amount of C and O is higher in the SEI of the lithium anode of oxygen cells.<sup>63,93</sup> The higher amount of C in the SEI seen in the oxygen cell compared to that in the non-oxygen cell is most likely due to an increase in the decomposition of PC solvent resulting from reactions with or catalyzed by the presence of oxygen.

More importantly, the changes in the surface composition of a lithium anode are shown in the XPS spectra in Figure 29, revealing that the composition of the SEI on lithium anode is evolving.

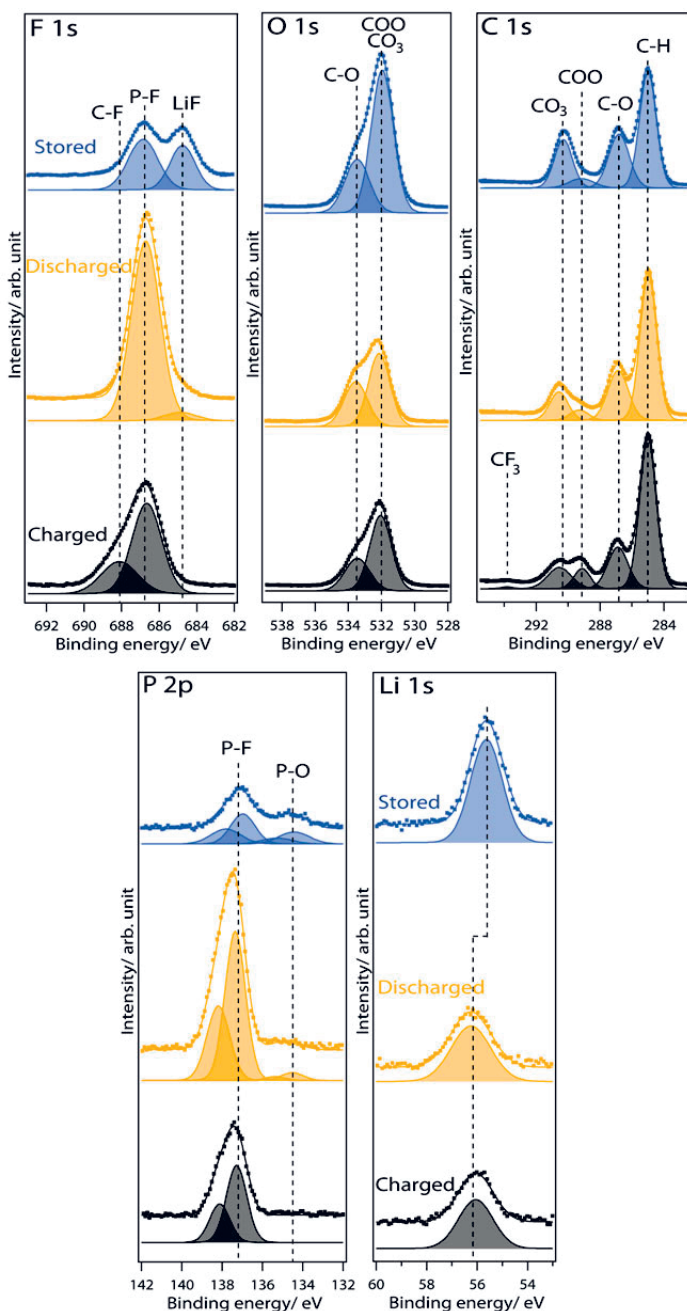
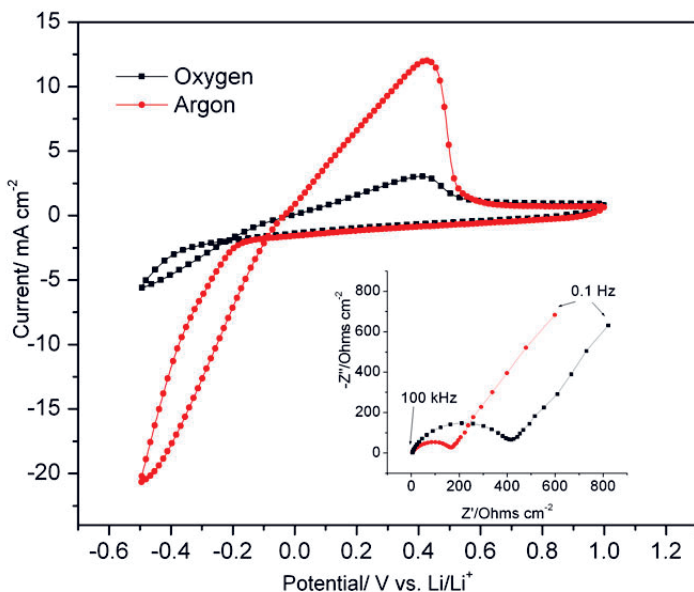


Figure 29. F 1s, O 1s, C 1s, P 2p, and Li 1s spectra of Li anode of stored (top), discharged (middle), and charged (bottom) Li-O<sub>2</sub> cells using 1 M LiPF<sub>6</sub> in PC.

To study the influence of oxygen on the electrochemical performance of a lithium anode, we investigated the lithium plating and stripping process on a copper surface in the presence and absence of oxygen. Figure 30 shows the

recorded CV measurement of the plating and stripping process. Compared to the Argon cell, the plating process starts at a significantly lower potential in the oxygen cell. The stripping process also stops at lower potential on the positive potential scan when compared to the oxygen cell. Thus, the CV results indicate higher resistance in the oxygen cell compared to the non-oxygen cell. The AC impedance of both oxygen and non-oxygen cells after the CV measurement is presented in the inset of Figure 30 indicating that the resistance in the presence of oxygen is higher compared to that of the non-oxygen cell.



*Figure 30.* Main: CV ( $100 \text{ mV s}^{-1}$ ) showing lithium deposition and stripping on Cu in the presence of oxygen and argon gas (the 3<sup>rd</sup> cycle in both cases). Inset: AC Impedance spectra recorded for both cells at 1 V vs. Li/Li<sup>+</sup> after 10 stripping and deposition cycles.



## 5. Concluding Remarks and Future Outlook

The aim of this thesis was to elucidate the reaction products in the relatively novel and complicated Li-O<sub>2</sub> battery and to determine the major parameters influencing the performance of the cell.

XPS in combination with synchrotron photoelectron spectroscopy were the main techniques used to characterize the surface of the electrodes to establish the composition of the reaction products. Gas adsorption and SEM were also used to investigate the porosity properties of the carbon cathodes.

Dividing the cell to the four main components, the following conclusions were ascertained in this study:

### **Cathode**

- The cathode formulation, specifically the relative amount of binder, influences the porosity properties including surface area, pore volume and pore size distribution of the cathode. In other words, surface and pore volume of carbon cathode decrease by increasing the relative amount of Kynar binder.
- The increase in relative amount of Kynar binder results in a decrease in the observed discharge capacity of the Li-O<sub>2</sub> battery.
- Kynar binder, which has commonly been used to assemble porous cathodes for use in Li-O<sub>2</sub> batteries, was found to degrade during cell cycling. Furthermore, it was shown that the decomposition products of ether electrolytes formed in contact with Li<sub>2</sub>O<sub>2</sub> in turn leads to the degradation of Kynar binder.
- As a consequence of the decomposition of the Kynar, LiF forms on the surface of the cathode, which can passivate the electroactive surface and catalysts. In addition, decomposition of Kynar may lead to degradation of the cathode structure and cause the blockage of the pores.

### **Electrolyte Solvent**

- Carbonate based solvents like PC and EC/DEC were found to be unstable during the cell cycling. The decomposition of these solvents to lithium carbonate, lithium alkyl carbonate, etc. results in the formation of a surface layer with a thickness of 5-10 nm on the carbon cathode, found by using XPS and HAXPES.
- Ether solvents such as TEGDME and PEGDME decompose during cell cycling forming ether based decomposition products.

- It was also shown that  $\text{Li}_2\text{O}_2$  decomposes all tested carbonate and ether solvents (PC, EC/DEC, and TEGDME). PC and EC/DEC form carbonate and PEO based compounds as a result of the reaction with  $\text{Li}_2\text{O}_2$ , while TEGDME forms carboxylate species.

### Electrolyte Salt

- $\text{LiPF}_6$ ,  $\text{LiB}(\text{CN})_4$  and LiBOB salt were shown to decompose during the cycling. These salts form LiF and B-O containing compounds which contribute to the formation of a surface layer on the carbon cathode.
- $\text{LiClO}_4$  salt dissolved in EC/DEC showed no decomposition product. However, this salt degraded to form LiCl during the cell cycling when PC was used as the solvent.
- The XPS results revealed that  $\text{LiPF}_6$ ,  $\text{LiBF}_4$  and  $\text{LiClO}_4$  salts decompose in contact with  $\text{Li}_2\text{O}_2$ , and consequently, form LiF, LiCl, and P-O containing compounds on the surface of  $\text{Li}_2\text{O}_2$ .
- The degradation of the electrolyte solvent and salt in contact with  $\text{Li}_2\text{O}_2$  results in the formation of a surface layer on  $\text{Li}_2\text{O}_2$ . Such a layer can passivate the surface of  $\text{Li}_2\text{O}_2$  leading to a charge overpotential in the cell.

### Anode

- Compared to a non-oxygen cell, in the  $\text{Li-O}_2$  battery in the presence of oxygen, PC decomposes to a higher degree on the lithium anode.
- The SEI on the lithium anode in a  $\text{Li-O}_2$  battery is evolving during the cell cycling.
- The cell resistance is higher in presence of oxygen than that in the absence of oxygen.
- The influence of the presence of oxygen on the formed SEI layer as well as the decomposition of the electrolyte by the lithium anode are issues which need to be studied further.

Overall, the presence of an oxygen atmosphere and oxygen ions in the cell makes the  $\text{Li-O}_2$  battery a very complicated system. Most common electrolyte solvents like organic carbonate and ether based solvents decompose in the  $\text{Li-O}_2$  battery. In addition, the degradation of most common Li salts such as  $\text{LiPF}_6$ ,  $\text{LiBF}_4$ , LiBOB, and  $\text{LiB}(\text{CN})_4$  has added more complexity. Although  $\text{LiClO}_4$  has in some cases more stability, it is not a practical Li salt due to safety issues.

Furthermore, the cross-talk between the components of  $\text{Li-O}_2$  battery complicates the system. This means that even if a stable electrolyte (possibly DMSO or polymer based electrolytes) is discovered, the long term stability of the electrolyte in contact with lithium anode in the presence of oxygen is a challenging issue. One suggested solution, however, is separating lithium anode from the electrolyte by using a solid membrane.

The difficulty in finding a stable electrolyte has to some degree hampered further studies of ORR and OER during long term cycling. As a consequence of this problem, further work to improve the cathode formulation, catalyst performance, and kinetics of the reactions are hindered.

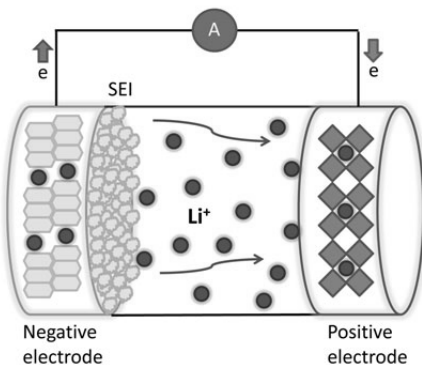
A useful approach to develop the Li-O<sub>2</sub> battery seems to be investigating each component of the cell individually. For example, to avoid the problems originating from employment of a lithium metal anode, nonmetallic anodes such as graphite or silicon can be used.

Considering all these difficulties, there is still a long way to go to produce Li-O<sub>2</sub> batteries for commercial scale.

# Sammanfattning på Svenska

Att öka mängden förnybar energi för att minska förbrukningen av fossila bränslen är ett viktigt mål i samhället. För att använda den elektricitet som kan skapas av vinden, vattnet eller solen, när det inte alltid blåser eller då solen inte alltid skiner, behövs effektiva energilagring. Batterier är en sådan lösning. Den globala uppvärmningen till följd av utsläpp av växthusgaser är ett av de viktigaste problemen att försöka lösa. Förutom att göra det genom att skapa mer förnybar energi måste också transportsektorn bli fossilfri och även här kan utvecklandet av avancerad energilagring såsom batterier spela en nyckelroll.

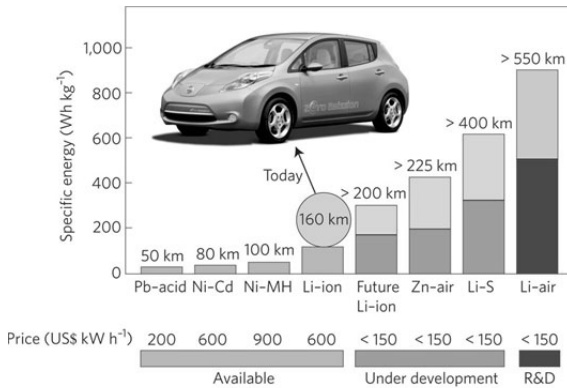
Ett batteri, eller en elektrokemisk cell, är tillverkad av elektroder och elektrolyt, som omvandlar kemisk energi till elektrisk energi, se Figur 1. Det moderna litiumjonbatteriet, som numera hittas i alla bärbara elektroniska apparater, är resultatet av många års forskning. Idag driver speciellt utvecklingen av elfordon batteriutvecklingen framåt. En ökning av både batteriets specifika energi (gravimetrisk energitäthet), energidensitet (volymetrisk energitäthet) och säkerhet samt att minska batteriets kostnad är de främsta målen.



Figur 1. Ett litium jonbatteri med interkalations elektroder.

När det gäller att kunna öka batteriers energitäthet har Li-O<sub>2</sub> batteriet (ofta kallat litium-luft batteriet) fått en särskild uppmärksamhet på senare år på grund av dess höga specifika energi. Denna typ av batteri har en teoretisk specifik kapacitet nästan 10 gånger högre än dagens interkalationsbaserade litium-jon batterier. Det förespås att ett fullt utvecklat Li-O<sub>2</sub> batteriet kommer ge en praktisk specifik kapacitet som är 2-3 gånger högre jämfört med dagens kommersiellt tillgängliga litiumjonbatterier (Figur 2).

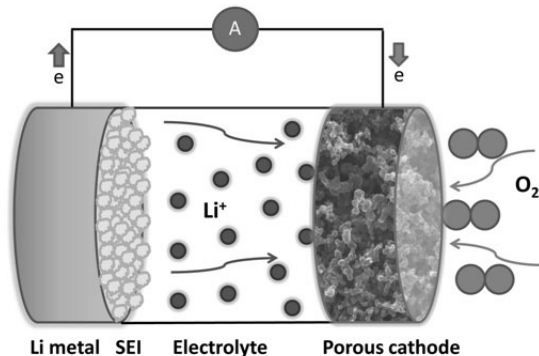
Li-O<sub>2</sub> batteriet består av en metallisk litumanod (eller möjligen en litiumlegering) och en porös katod, och mellan dem finns det en separator innehållande elektrolyt, se schematisk bild i Figur 3. Under urladdning av Li-O<sub>2</sub> batteriet transporteras litiumjoner genom elektrolyten från anoden till katoden där de kan reagera med syre från luften.



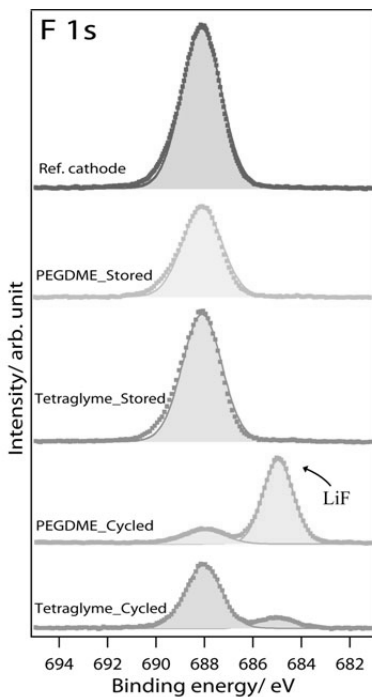
Figur 2. Jämförelse vad gäller energitätheter hos olika uppladdningsbara batterier.

I denna avhandling har Li-O<sub>2</sub> batteriet studerats för att belysa de komplicerade parametrar som påverkar systemets funktion. Avhandlingen syftar till att ge ökad förståelse av de reaktioner som sker under cykling och vidare bestämma vilka reaktionsprodukterna är som bildas vid cykling. Avhandlingen innehåller resultat från studier av de tre största cellkomponenterna, dvs katod, anod och elektrolyt i cellen. Flera karakteriseringstekniker inklusive fotoelektron spektroskopi (XPS), svepelektron mikroskopi (SEM), röntgendiffraktion (XRD) och gasadsorption har använts för att analysera cellelektroden tillsammans med elektrokemiska mätningar av Li-O<sub>2</sub>-celler. Särskilt har gränzytorna mellan elektrod och elektrolyt studerats i detta arbete eftersom det är här nerbrytningsprocesserna sker. Ytkarakterisering av både kolkatoden och litiumanoden i battericellerna har studerats med XPS. Detta har varit en utmaning då skikten som bildas i gränzytorna är väldigt tunna (ca 5 nanometer) och väldigt känsliga för luft (syre och vatten).

En av de parametrar som har undersökts systematiskt i avhandlingen var porositeten hos katoden och hur den kopplas till batteriets urladdningskapacitet. Resultaten visar att ytarean och porvolymen hos katoderna minskar med ökande mängd av Kynar bindemedel (som behövs för att hålla ihop elektrodpulvret). En tillsats av 20 vikt-% av Kynar reducerar ytarean och porvolymen med ca 30% respektive 20%, jämfört med Super P kol. Det faktum att den högsta kapaciteten vid första urladdningen erhöles med den lägsta mängden av Kynar bindemedel i katoden bekräftar att den porositet som katoden har till stor del påverkar urladdningskapaciteten hos cellen.



Figur 3. En schematisk bild av Li-O<sub>2</sub>-batteriet.



Figur 4. F 1s spektra av referenskatod, ocyklad and cyklad Li-O<sub>2</sub>-batterikatod. Dessa katoder är cyklade med en elektrolyt bestående av LiB(CN)<sub>4</sub> i PEGDME eller Tetraglyme.

bindemedlet som därför i sin tur sönderfaller. De nedbrytningsprodukter som bildades i kontakt med Li<sub>2</sub>O<sub>2</sub> vid användning av karbonatlösningemedel såsom PC (polyvinylkarbonat) i elektrolyten är dock inte reaktiva mot Kynar-bindemedlet.

Alla elektrolyter för litiumjonbatterier eller Li-O<sub>2</sub>-batterier består av ett lösningsmedel och ett litiumsalt. De redan beskrivna resultaten antydde att lösningsmedlet inte var stabilt i Li-O<sub>2</sub> batteriet under cykling. Därför studerades flera olika lösningsmedel i detalj för att förstå vilka parametrar som påverkar stabiliteten. Några av resultaten är sammanfattade i följande punkter:

- Karbonatlösningemedel såsom PC eller EC/DEC sönderdelas under urladdningen av Li-O<sub>2</sub>-batterier då de reagerar med reducerade syrejoner eller på grund av reaktioner med urladdningsprodukten Li<sub>2</sub>O<sub>2</sub>.

Vidare visar XPS resultat att Kynar bindemedlet i vissa fall är instabilt i Li-O<sub>2</sub>-batteriet. Mängden fluor som finns på ytan kan mätas i PES F 1s toppen. Den avslöjar närvaron av LiF på ytan av de cyklade katoderna, medan ocyklade elektroder som lagrats i elektrolyt endast innehåller fluor som kommer från Kynar, se Figur 4. I dessa batterier användes en katod som består av Kynar tillsammans med Super P kol och katalysatorn  $\alpha$ -MnO<sub>2</sub>, och batterierna blev galvanostatiskt cyklade med eterbaserade elektrolyter: 0,5 M LiB(CN)<sub>4</sub> i TEGDME eller PEGDME. Eftersom icke-fluorerade elektrolyter användes i denna studie, är Kynar bindemedlet den enda källan för fluor. Närvaro av LiF på ytan hos de cyklade katoderna indikerar därför att Kynar bindemedlet sönderdelas.

Den kemiska stabiliteten hos katodkomponenter i kontakt med en av de föreslagna urladdnings produkterna Li<sub>2</sub>O<sub>2</sub> undersöktes också. XPS resultaten antyder att lösningsmedlet eter såsom TEGDME och DME sönderdelas kemiskt i kontakt med Li<sub>2</sub>O<sub>2</sub> och att nedbrytningsprodukterna i sin tur reagerar med Kynar

- Sönderdelningen av PC eller EC/DEC resulterar i bildandet av ~ 5 till 10 nm tjocka ytskikt som passiverar ytan på katoden och på MnO<sub>2</sub> katalysatorn.
- Eterlösningsmedel såsom TEGDME och PEGDME försämras under cellcykelförloppet på grund av reaktioner med reducerade syrejoner.
- Alla testade karbonat- och eter lösningsmedel (PC, EC/DEC, TEGDME) var instabila i direkt kontakt med Li<sub>2</sub>O<sub>2</sub>.

Stabiliteten hos salterna som sådana studerades också.

- Salter av LiPF<sub>6</sub>, LiB(CN)<sub>4</sub>, och LiBOB var alla instabila under cykling av Li-O<sub>2</sub>-celler.
- LiClO<sub>4</sub> visade ingen nedbrytningsprodukt på kolkatoden i en cell som cyklade med EC/DEC men i PC-elektrolyt sönderdelades LiClO<sub>4</sub> till LiCl.
- Salternas nedbrytningsprodukter bidrog till bildandet av ytskikt på kolkatoden.
- LiPF<sub>6</sub>, LiBF<sub>4</sub> och LiClO<sub>4</sub> befanns vara instabila i kontakt med Li<sub>2</sub>O<sub>2</sub> vilket ledde till bildandet av nedbrytningsprodukter såsom LiF, LiCl och PO-föreningar på ytan av Li<sub>2</sub>O<sub>2</sub>.

Det är hittills ingen som studerat vad som egentligen bildas på litiumelektroden när ett Li-O<sub>2</sub> batteri cyklar. Några av de viktigaste resultaten från denna avhandling är därför:

- PC sönderdelas till en högre grad på litiumanoden i ett Li-O<sub>2</sub> batteri i närvaro av syre än vad som sker i ett ”syrefritt” batteri.
- SEI på litiumanoden i ett Li-O<sub>2</sub> batteri under batteriets cykling.
- Motståndet i cellen är högre i närvaro av syre än i frånvaro av syre.
- Vad som egentligen sker i närvaro av syre för det bildade ytskiktet (SEI) på litiumanoden behöver studeras ytterligare.

Denna avhandling visar att för att få ett fungerande uppladdningsbart Li-O<sub>2</sub> batteri måste litiumanoden skyddas från vatten och syre, nya elektrolytssystem (både lösningsmedel och salter) behöver utvecklas samt också nya katalysatorer som är miljövänliga och billiga och som leder till att reaktionsprodukten Li<sub>2</sub>O<sub>2</sub> kan reagera så att syre återbildas och litiumjoner reduceras till metalliskt litium. Det är en utmaning att göra att fungerande Li-O<sub>2</sub>-batteri.

# Acknowledgements

First of all, I would like to thank my supervisor Professor Kristina Edström. I am deeply indebted and thankful for all your continual support during this PhD work. Thanks a lot Kristina for all your patience. I will never forget your help and kindness.

I would also like to thank Patrik Johansson and Fredrik Björefors for all your comments on my work and papers. Thank you Patrik, for all your quick replies and your enthusiasm about the work. Thank you Fredrik, for always being open for almost daily short chats. Torbjörn Gustafsson, Leif Nyholm, and Josh Thomas, thanks for your comments on this work and sharing your knowledge with me. Yvonne, I'm grateful to you for your help and support.

Special thanks to Maria, Matthew, and Sigita for introducing me to new fields. I have learned many new things from you. It was kind of you Maria to show me carefully how to work with our in house XPS and in synchrotron facilities at Maxlab and BESSY. Thank you Matthew, for all your valuable comments and daily scientific, nonscientific discussions and chats and also for your non-ending positive energy to projects. It was very great to work and discuss with you and to think about many new ideas and projects.

A big thanks to all colleagues and friends in the battery and fuel cell group: Adam, Andreas, Anti, Bertrand, Bing, Cesar, Chao, Daniel, David, Fredrik, Gabi, Girma, Habtom, Jeff, Jia, Jonas H., Jonas M., Karima, Kasia, Mario, Matt, Mohammed, Rickard, Sara Ma., Sara Mu., Steven, Taha, Wei Wei, Wendy and Will. Thanks a lot for contributing to the fun times and making a such nice atmosphere in the lab, for all scientific and nonscientific collaborations, for having lunch and coffee together, playing football, going to conferences and trips together, for teasing you, for “potatis”, and ...I should also thank some former colleagues whom I had nice times with: Cip-tanti, David, Emilie, Hanna, Ida, Kinson, Ji, Mirjana, Neelam, Semra, Ser-dar, Tanguy, and...Thanks to my roomies, Anna and Song. It was a pleasure to share an office with you.

A big thank you to Henrik for all your assistances in the lab, for arranging things to work and making a nice atmosphere within the lab. Also, a thank you from my “fishes” for all your advice... I would like to express gratitude towards Tatti, Eva, Anders, and Peter for all your help.

And, thanks to all people in structural and inorganic chemistry groups for making a very nice atmosphere in the department.



I would like to thank in a greater context than science to my family, relatives and friends. Special thanks to my parents, brother and sister for all your love and support. Thanks to my parents in law, and to Shahryar and Farnaz. Thanks to Alireza, Mehrdad, Nasrolah, Sajad, Taher, their families and all Iranian friends in Uppsala, Stockholm and in the rest of Sweden for your friendship and support.

Last but not least a big thank you with love to my wife, Sahar. Thank you for understanding me, for your kindness and your patience in difficult times, and for all your support. It would be much more difficult to finish this work without you.

# References

- (1) Smil, V. *Energy at the crossroads*; The MIT Press, 2003.
- (2) *Energy in Sweden 2011*; Swedish Energy Agency, 2011.
- (3) *Energy Indicators 2009*; Swedish Energy Agency, 2009.
- (4) Klare, M. *Blood and Oil*; Penguin Group, 2005.
- (5) Froom, A. Riddle of “Baghdad”’s batteries  
<http://news.bbc.co.uk/2/hi/science/nature/2804257.stm>.
- (6) Palacin, M. R. *Chemical Society Reviews* **2009**, *38*, 2565–2575.
- (7) Xu, K. *Chemical Reviews* **2004**, *104*, 4303–4418.
- (8) Huggins, R. A. *Advanced Batteries*; Springer US: Boston, MA, 2009.
- (9) Bruce, P. G.; Freunberger, S. A.; Hardwick, L. J.; Tarascon, J.-M. *Nature Materials* **2011**, *11*, 19–29.
- (10) Christensen, J.; Albertus, P.; Sanchez-Carrera, R. S.; Lohmann, T.; Kozinsky, B.; Liedtke, R.; Ahmed, J.; Kojic, A. *Journal of The Electrochemical Society* **2012**, *159*, R1.
- (11) Abraham, K. M.; Jiang, Z. *Journal of The Electrochemical Society* **1996**, *143*, 1–5.
- (12) Ogasawara, T.; Débart, A.; Holzapfel, M.; Novák, P.; Bruce, P. G. *Journal of the American Chemical Society* **2006**, *128*, 1390–1393.
- (13) Débart, A.; Bao, J.; Armstrong, G.; Bruce, P. G. *Journal of Power Sources* **2007**, *174*, 1177–1182.
- (14) Débart, A.; Paterson, A. J.; Bao, J.; Bruce, P. G. *Angewandte Chemie International Edition* **2008**, *47*, 4521–4524.
- (15) Laroire, C. O.; Mukerjee, S.; Abraham, K. M.; Plichta, E. J.; Hendrickson, M. A. *The Journal of Physical Chemistry C* **2010**, *114*, 9178–9186.
- (16) Laroire, C. O.; Mukerjee, S.; Abraham, K. M.; Plichta, E. J.; Hendrickson, M. A. *The Journal of Physical Chemistry C* **2009**, *113*, 20127–20134.
- (17) Shao, Y.; Park, S.; Xiao, J.; Zhang, J.-G.; Wang, Y.; Liu, J. *ACS Catalysis* **2012**, *2*, 844–857.
- (18) Cao, R.; Lee, J.-S.; Liu, M.; Cho, J. *Advanced Energy Materials* **2012**, *2*, 816–829.
- (19) Cheng, F.; Chen, J. *Chemical Society Reviews* **2012**, *41*, 2172–2192.
- (20) Suntivich, J.; Gasteiger, H. a; Yabuuchi, N.; Nakanishi, H.; Goodenough, J. B.; Shao-Horn, Y. *Nature Chemistry* **2011**, *3*, 546–50.
- (21) Cui, Y.; Wen, Z.; Liu, Y. *Energy & Environmental Science* **2011**, *4*, 4727.
- (22) Mitchell, R. R.; Gallant, B. M.; Thompson, C. V.; Shao-Horn, Y. *Energy & Environmental Science* **2011**, *4*, 2952–2958.
- (23) Tran, C.; Kafle, J.; Yang, X.-Q.; Qu, D. *Carbon* **2011**, *49*, 1266–1271.
- (24) Kuboki, T.; Okuyama, T.; Ohsaki, T.; Takami, N. *Journal of Power Sources* **2005**, *146*, 766–769.
- (25) Xiao, J.; Wang, D.; Xu, W.; Wang, D.; Williford, R. E.; Liu, J.; Zhang, J.-G. *Journal of The Electrochemical Society* **2010**, *157*, A487.
- (26) Read, J. *Journal of The Electrochemical Society* **2002**, *149*, A1190.

- (27) Mirzaeian, M.; Hall, P. J. *Electrochimica Acta* **2009**, *54*, 7444–7451.
- (28) Yang, X.; He, P.; Xia, Y. *Electrochemistry Communications* **2009**, *11*, 1127–1130.
- (29) Tran, C.; Yang, X.-Q.; Qu, D. *Journal of Power Sources* **2010**, *195*, 2057–2063.
- (30) Younesi, S. R.; Urbonaitė, S.; Björefors, F.; Edström, K. *Journal of Power Sources* **2011**, *196*, 9835–9838.
- (31) Freunberger, S. A.; Chen, Y.; Peng, Z.; Griffin, J. M.; Hardwick, L. J.; Bardé, F.; Novák, P.; Bruce, P. G. *Journal of the American Chemical Society* **2011**, *133*, 8040–8047.
- (32) Mizuno, F.; Nakanishi, S.; Kotani, Y.; Yokoishi, S.; Iba, H. *Electrochemistry* **2010**, *78*, 403–405.
- (33) Younesi, R.; Urbonaitė, S.; Edström, K.; Hahlin, M. *The Journal of Physical Chemistry C* **2012**, *116*, 20673–20680.
- (34) Gibian, M. J.; Sawyer, D. T.; Ungermann, T.; Tangpoonpholvivat, R.; Morrison, M. M. *Journal of the American Chemical Society* **1979**, *101*, 640–644.
- (35) Xu, W.; Xu, K.; Viswanathan, V. V.; Towne, S. A.; Hardy, J. S.; Xiao, J.; Nie, Z.; Hu, D.; Wang, D.; Zhang, J.-G. *Journal of Power Sources* **2011**, *196*, 9631–9639.
- (36) Bryantsev, V. S.; Blanco, M. *The Journal of Physical Chemistry Letters* **2011**, *2*, 379–383.
- (37) Laino, T.; Curioni, A. *Chemistry – A European Journal* **2012**, *18*, 3510–3520.
- (38) Younesi, R.; Hahlin, M.; Björefors, F.; Johansson, P.; Edström, K. *to be published*.
- (39) Sawyer, D. T.; Valentine, J. S. *Accounts of Chemical Research* **1981**, *14*, 393–400.
- (40) Veith, G. M.; Dudney, N. J.; Howe, J.; Nanda, J. *The Journal of Physical Chemistry C* **2011**, *115*, 14325–14333.
- (41) Laire, C. O.; Mukerjee, S.; Plichta, E. J.; Hendrickson, M. A.; Abraham, K. M. *Journal of The Electrochemical Society* **2011**, *158*, A302.
- (42) McCloskey, B. D.; Bethune, D. S.; Shelby, R. M.; Girishkumar, G.; Luntz, A. C. *The Journal of Physical Chemistry Letters* **2011**, *2*, 1161–1166.
- (43) Jung, H.-G.; Hassoun, J.; Park, J.-B.; Sun, Y.-K.; Scrosati, B. *Nature Chemistry* **2012**, *4*, 579–585.
- (44) Wang, Z.-L.; Xu, D.; Xu, J.-J.; Zhang, L.-L.; Zhang, X.-B. *Advanced Functional Materials* **2012**, *22*, 3699–3705.
- (45) Li, Y.; Wang, J.; Li, X.; Geng, D.; Norouzi Banis, M.; Tang, Y.; Wang, D.; Li, R.; Sham, T.-K.; Sun, X. *Journal of Materials Chemistry* **2012**, *22*, 20170–20174.
- (46) Wang, H.; Xie, K. *Electrochimica Acta* **2012**, *64*, 29–34.
- (47) Freunberger, S. A.; Chen, Y.; Drewett, N. E.; Hardwick, L. J.; Bardé, F.; Bruce, P. G. *Angewandte Chemie International Edition* **2011**, *50*, 8609–8613.
- (48) Younesi, R.; Hahlin, M.; Treskow, M.; Scheers, J.; Johansson, P.; Edström, K. *The Journal of Physical Chemistry C* **2012**, *116*, 18597–18604.
- (49) Veith, G. M.; Nanda, J.; Delmau, L. H.; Dudney, N. J. *The Journal of Physical Chemistry Letters* **2012**, *3*, 1242–1247.
- (50) Hyoungh Oh, S.; Yim, T.; Pomerantseva, E.; Nazar, L. F. *Electrochemical and Solid-State Letters* **2011**, *14*, A185.
- (51) Oswald, S.; Mikhailova, D.; Scheiba, F.; Reichel, P.; Fiedler, A.; Ehrenberg, H. *Analytical and Bioanalytical Chemistry* **2011**, *400*, 691–6.

- (52) McCloskey, B. D.; Speidel, A.; Scheffler, R.; Miller, D. C.; Viswanathan, V.; Hummelshøj, J. S.; Nørskov, J. K.; Luntz, A. C. *The Journal of Physical Chemistry Letters* **2012**, *3*, 997–1001.
- (53) Chalasani, D.; Lucht, B. L. *ECS Electrochemistry Letters* **2012**, *1*, A38–A42.
- (54) Aurbach, D. *Nonaqueous Electrochemistry*; Marcel Dek.: New York, 1999.
- (55) Rauh, R. D.; Brummer, S. B. *Electrochimica Acta* **1977**, *22*, 75–83.
- (56) Aurbach, D.; Zaban, A.; Gofar, Y.; Ely, Y. E.; Weissman, I.; Chusid, O.; Abramson, O. *Journal of Power Sources* **1995**, *54*, 76–84.
- (57) Jesse, T. M. A. and A. K. and S. V. K. and S. *Nanotechnology* **2012**, *23*, 325402.
- (58) Visco, S. J.; Katz, B. D.; Nimon, Y. S.; Jonghe, L. C. D. Protected active metal electrode and battery cell structures with non-aqueous interlayer architecture **2007**.
- (59) Zhang, T.; Imanishi, N.; Hasegawa, S.; Hirano, A.; Xie, J.; Takeda, Y.; Yamamoto, O.; Sannes, N. *Electrochemical and Solid-State Letters* **2009**, *12*, A132–A135.
- (60) Hasegawa, S.; Imanishi, N.; Zhang, T.; Xie, J.; Hirano, A.; Takeda, Y.; Yamamoto, O. *Journal of Power Sources* **2009**, *189*, 371–377.
- (61) McCloskey, B. D.; Bethune, D. S.; Shelby, R. M.; Mori, T.; Scheffler, R.; Speidel, A.; Sherwood, M.; Luntz, A. C. *The Journal of Physical Chemistry Letters* **2012**, *3*, 3043–3047.
- (62) Hassoun, J.; Jung, H.-G.; Lee, D.-J.; Park, J.-B.; Amine, K.; Sun, Y.-K.; Scrosati, B. *Nano Letters* **2012**.
- (63) Younesi, R.; Hahlin, M.; Roberts, M.; Edström, K. *Journal of Power Sources* **2013**, *225*, 40–45.
- (64) Girishkumar, G.; McCloskey, B.; Luntz, A. C.; Swanson, S.; Wilcke, W. *The Journal of Physical Chemistry Letters* **2010**, *1*, 2193–2203.
- (65) Kraysberg, A.; Ein-Eli, Y. *Journal of Power Sources* **2011**, *196*, 886–893.
- (66) Hardwick, L. J.; Bruce, P. G. *Current Opinion in Solid State and Materials Science* **2012**, *16*, 178–185.
- (67) Padbury, R.; Zhang, X. *Journal of Power Sources* **2011**, *196*, 4436–4444.
- (68) Park, M.; Sun, H.; Lee, H.; Lee, J.; Cho, J. *Advanced Energy Materials* **2012**, *2*, 780–800.
- (69) Peng, Z.; Freunberger, S. A.; Chen, Y.; Bruce, P. G. *Science* **2012**, *337*, 563–566.
- (70) Peng, Z.; Freunberger, S. A.; Hardwick, L. J.; Chen, Y.; Giordani, V.; Bardé, F.; Novák, P.; Graham, D.; Tarascon, J.-M.; Bruce, P. G. *Angewandte Chemie International Edition* **2011**, *50*, 6351–6355.
- (71) Schnadt, J.; Knudsen, J.; Andersen, J. N.; Siegbahn, H.; Pietzsch, A.; Hennies, F.; Johansson, N.; Mårtensson, N.; Ohrwall, G.; Bahr, S.; Mähl, S.; Schaff, O. *Journal of Synchrotron Radiation* **2012**, *19*, 701–704.
- (72) Lu, Y.-C.; Crumlin, E. J.; Veith, G. M.; Harding, J. R.; Mutoro, E.; Baggetto, L.; Dudney, N. J.; Liu, Z.; Shao-Horn, Y. *Scientific Reports* **2012**, *2*, 715.
- (73) van der Heide, P. *X-ray Photoelectron Spectroscopy*; X-ray Photoelectron Spectroscopy; John Wiley & Sons, Ltd, 2012.
- (74) Hüfner, S. *Photoelectron Spectroscopy*; 3rd ed.; Springer, **2003**.
- (75) Pijolat, M.; Hollinger, G. *Surface Science* **1981**, *105*, 114–128.
- (76) Seah, M. P. *Surface and Interface Analysis* **2012**, *44*, 497–503.
- (77) Gorgoi, M.; Svensson, S.; Schäfers, F.; Ohrwall, G.; Mertin, M.; Bressler, P.; Karis, O.; Siegbahn, H.; Sandell, A.; Rensmo, H.; Doherty, W.; Jung, C.; Braun, W.; Eberhardt, W. *Nuclear Instruments and Methods in Physics Re-*

- search Section A: Accelerators, Spectrometers, Detectors and Associated Equipment* **2009**, 601, 48–53.
- (78) Read, J.; Mutolo, K.; Ervin, M.; Behl, W.; Wolfenstine, J.; Driedger, a.; Foster, D. *Journal of The Electrochemical Society* **2003**, 150, A1351–A1356.
- (79) Morita, M.; Niida, Y.; Yoshimoto, N.; Adachi, K. *Journal of Power Sources* **2005**, 146, 427–430.
- (80) Black, R.; Oh, S. H.; Lee, J.-H.; Yim, T.; Adams, B.; Nazar, L. F. *Journal of the American Chemical Society* **2012**, 134, 2902–2905.
- (81) Wade, L. G. *Organic Chemistry*; 7th ed.; Pearson Prentice Hall, 2010.
- (82) Xu, W.; Hu, J.; Engelhard, M. H.; Towne, S. A.; Hardy, J. S.; Xiao, J.; Feng, J.; Hu, M. Y.; Zhang, J.; Ding, F.; Gross, M. E.; Zhang, J.-G. *Journal of Power Sources* **2012**, 215, 240–247.
- (83) Zhang, Z.; Lu, J.; Assary, R. S.; Du, P.; Wang, H.-H.; Sun, Y.-K.; Qin, Y.; Lau, K. C.; Greeley, J.; Redfern, P. C.; Iddir, H.; Curtiss, L. A.; Amine, K. *The Journal of Physical Chemistry C* **2011**, 115, 25535–25542.
- (84) Bryantsev, V. S.; Giordani, V.; Walker, W.; Blanco, M.; Zecevic, S.; Sasaki, K.; Uddin, J.; Addison, D.; Chase, G. V. *The Journal of Physical Chemistry A* **2011**, 115, 12399–12409.
- (85) Ashley, A. J. C. *Radiation Research* **1982**, 90, 433–436.
- (86) Cota, L. G.; de la Mora, P. *Acta crystallographica. Section B, Structural science* **2005**, 61, 133–136.
- (87) Zhang, X.; Kostecki, R.; Richardson, T. J.; Pugh, J. K.; Ross, P. N. *Journal of The Electrochemical Society* **2001**, 148, A1341–A1345.
- (88) Aurbach, D.; Daroux, M. L.; Faguy, P. W.; Yeager, E. *Journal of The Electrochemical Society* **1987**, 134, 1611–1620.
- (89) Andersson, A. M.; Edström, K. *Journal of The Electrochemical Society* **2001**, 148, A1100–A1109.
- (90) Scheers, J.; Pitawala, J.; Thebault, F.; Kim, J.-K.; Ahn, J.-H.; Matic, A.; Johansson, P.; Jacobsson, P. *Physical Chemistry Chemical Physics* **2011**, 13, 14953–14959.
- (91) Clover, A. M. *Journal of the American Chemical Society* **1922**, 44, 1107–1118.
- (92) Nazri, G.; Muller, R. H. *Journal of The Electrochemical Society* **1985**, 132, 2050–2054.
- (93) Aurbach, D.; Weissman, I.; Schechter, A.; Cohen, H. *Langmuir* **1996**, 12, 3991–4007.

# Acta Universitatis Upsaliensis

*Digital Comprehensive Summaries of Uppsala Dissertations  
from the Faculty of Science and Technology 1001*

Editor: The Dean of the Faculty of Science and Technology

A doctoral dissertation from the Faculty of Science and Technology, Uppsala University, is usually a summary of a number of papers. A few copies of the complete dissertation are kept at major Swedish research libraries, while the summary alone is distributed internationally through the series Digital Comprehensive Summaries of Uppsala Dissertations from the Faculty of Science and Technology.



ACTA  
UNIVERSITATIS  
UPSALIENSIS  
UPPSALA  
2012

Distribution: [publications.uu.se](http://publications.uu.se)  
urn:nbn:se:uu:diva-183887